Received October 31, 2020, accepted November 4, 2020, date of publication November 9, 2020, date of current version November 20, 2020.

Digital Object Identifier 10.1109/ACCESS.2020.3036898

A Social Beetle Swarm Algorithm Based on Grey Target Decision-Making for a Multiobjective Distribution Network Reconfiguration Considering Partition of Time Intervals

QIAN CHEN[1], WEIQING WANG[1], HAIYUN WANG[1], JIAHUI WU[1], XIAOZHU LI[1], AND JIONGFENG LAN[2]

[1]Engineering Research Center of Education Ministry for Renewable Energy Power Generation and Grid-connected Control, Xinjiang University, Urumqi 830047, China

[2]Business School, Newcastle University, Newcastle NE1 4SE, U.K.

Corresponding author: Weiqing Wang (wwweiqing10101010@163.com)

This work was supported in part by the National Natural Science Foundation of China under Grant 51667020, in part by the Autonomous Region Government under Grant 2018D04005, in part by the Xinjiang Autonomous Region under Grant XJEDU2019I009, and in part by the Ministry of Education under Grant IRT-16R63.

ABSTRACT With the increased distributed generation (DG) and the combination of residential, commercial, and industrial loads connected to the distribution networks, it is more difficult to ensure the safe and economic operation of the distribution networks because of the great volatility and randomness of DG and complex loads. In this paper, with the aim of minimizing network loss, load balance, and maximum voltage deviation, a multiobjective reconfiguration model of the distribution network is established under the condition of satisfying network constraints. Moreover, a new social beetle swarm optimization algorithm (SBSO) considering two social behaviors is adopted to solve the complex problem according to the characteristics of the distribution network reconfiguration (DNRC). Based on the SBSO algorithm, grey target decision-making (GTDM) strategy is used to choose the best beetle in the process of solving the multiobjective problem. Additionally, The grey relation projection (GRP) method is used to divide the time period of DNRC according to the change of DG and loads in a day, in order to reduce the number of switching operations. Finally, the effectiveness of the proposed multiobjective model and algorithm are verified on the standard IEEE-33 system and IEEE-69 system.

INDEX TERMS Distribution network reconfiguration, multiobjective optimization, grey target decision-making strategy, grey relation projection, SBSO algorithm.

I. INTRODUCTION

DNRC is used to change the topological structure of the distribution network by changing the state of switches under the condition of satisfying network constraints, thereby enhancing the efficiency and stability of the distribution network [1], so the DNRC has been considered a powerful tool in distribution system planning and operation. In the DNRC problem, we determine the optimal radial configuration, the close/open status of each branch equipped with a controllable switch, on the given meshed distribution system for different objectives [2], [3]. At present, with the large-scale renewable energy interconnection and the combination of residential, commercial, and industrial loads, the distribution network has become more and more complex. Its randomness and volatility will bring challenges for the safety and economy of traditional distribution networks [4]. In addition, DG into distribution networks is implemented for reducing network losses, balancing demand overloads, improving the node voltage level, and absorbing renewable energy [5], which further increases the complexity of the distribution network. Therefore, it is necessary to perform research on this issue.

In the process of DNRC, many scholars have investigated network reconfiguration with different objectives and

The associate editor coordinating the review of this manuscript and approving it for publication was Fabio Massaro.

algorithms. [6], [7] study DNRC with the single objective of minimizing active power loss of the distribution network. Other researchers focused on double objectives of reducing the network loss and voltage deviation [8]. In addition, in order to ensure that the load in the power grid is not overloaded, Jakus established a mathematical model about DNRC with the aim of minimizing active power loss and load balance [9]. However, with more and more DG and complex loads connected to the power grid, the distribution network has become increasingly complicated for the operational control of the distribution network [10]. The dynamic changes of renewable and load are not taken into account in these models. In fact, wind power and photovoltaic power change with wind speed and solar radiation, respectively, and the wind speed and solar radiation can be simulated by the Weibull distribution [11] and beta distribution [12], [13]. The model of distribution network reconfiguration considering these uncertainties is built in [14], [15], but the load time variation is not considered. Although the uncertain variables of DG output and loads are considered in [1], the model is a single objective only considered.

Simultaneously, based on DG and load time variation, the main method of dynamic reconfiguration is to segment the time according to the change of DG and load in a day, and the number of switching operations can be greatly reduced by dividing the reconfiguration period. The dynamic reconfiguration method based on information entropy of time intervals is put forward in [16]. [17] proposed the index of power moment, and the power moment imbalance is compared with the predetermined power moment threshold. The interval that satisfies the requirement is merged into the last period to complete the partition of time intervals. In addition, [18] takes the monotone interval's integral median point of the load curve as a piecewise point and combines the adjacent intervals which have the minimum load decline until the preset partition number is reached. The improved fuzzy mean clustering algorithm is applied in [19] for the partition of time intervals, and the value of the combined loss function is used to determine the optimal partition number and plan. However, the dynamic reconstruction methods put forward in these references all need parameters such as preset partition number or comparison threshold, which have partly human subjectivity, on the other hand, these methods are complex and time-consuming, a high computational cost cannot be avoided.The GRP method is widely used in the correlation analysis of sequence, which is simple and efficient. For example, [20]–[22] uses GRP method to obtain the 'best' compromise solutions by calculating the priority memberships of the solutions. However, this useful method is not utilized to divide the reconfiguration period.

Additionally, when solving multiobjective optimization problems, the multiobjective is usually weighted and converted into a single objective. This processing process is relatively rough, and the three objectives cannot be optimized at the same time. Therefore, some scholars use the double-layer model to address multiobjectives [23]. Other scholars introduced the game theory and constructed a multiobjective game model [24] to solve the multiobjective problem. At the same time, the Pareto optimal solution is widely used in solving multiobjective optimization problems [25]–[27]. However, the Pareto optimal solution is only an acceptable solution set of the problem, and there are multiple Pareto optimal solutions in general. At this time, people need to make their own decisions, which is not objective. For this problem, [28] separates the obtained Pareto-optimal solutions(POSs) into different clusters and thereupon identifies the best compromise solutions (BCSs) by assessing the relative projections of the solutions belonging to the same cluster using GRP. The multiobjective GTDM can select a satisfactory scheme without losing objectivity. Professor Deng Julong, a Chinese scholar, founded the grey system theory in 1982 [29]. After that, the grey theory has been widely used and a series of grey decision-making methods have been produced, it is an effective decision-making method. GTDM not only helps people to make an objective decision, but also effectively solves multiobjective optimization problems with the heuristic algorithm in recent years. A GTDM theory based on the entropy weight method is proposed in [30] to identify the best trade off scheduling scheme among all the solutions. [31] integrated decision-making by combining the fuzzy c-means algorithm (FCM) with GRP aims to extract the best compromise solutions which reflect the preferences of decisionmakers from the POSs. However, these algorithms are easily affected by the parameters, and the solution is unstable. In 2017, the beetle antennae search (BAS) was proposed as an efficient and intelligent search algorithm [32]. The BAS algorithm does not need to know the specific form of the search, which is simple and efficient. However, in each iteration, the convergence result of the BAS algorithm depends on the direction of the beetle, which has great randomness [33]. To solve these problems, particle swarm optimization (PSO) [34] and BAS are combined to form the beetle swarm optimization (BSO) algorithm. At present, the BSO algorithm and grey decision method are not effectively combined to solve multiobjective optimization problems. Here, this paper uses a BSO algorithm based on GTDM to solve the problem of multiobjective optimal network reconfiguration. Furthermore, to improve the efficiency of optimization, the search speed of the global optimal solution is accelerated by changing its operator, increasing social learning behavior, and sorting after each iteration. On this basis, this paper uses SBSO algorithm combined GTDM to solve the multiobjective model to reduce the calculation time through the individual advantage of the beetle and this method is effective to avoid volatility and subjectivity.

The main contributions of this paper are as follows:

1 To avoid the high computational cost, the GRP method is used to analyze the net load of the distribution network to divide the time period of DNRC without human subjectivity.

2 A new modified SBSO algorithm considering two social behaviors is presented to determine the best configuration, in order to improve the search efficiency.

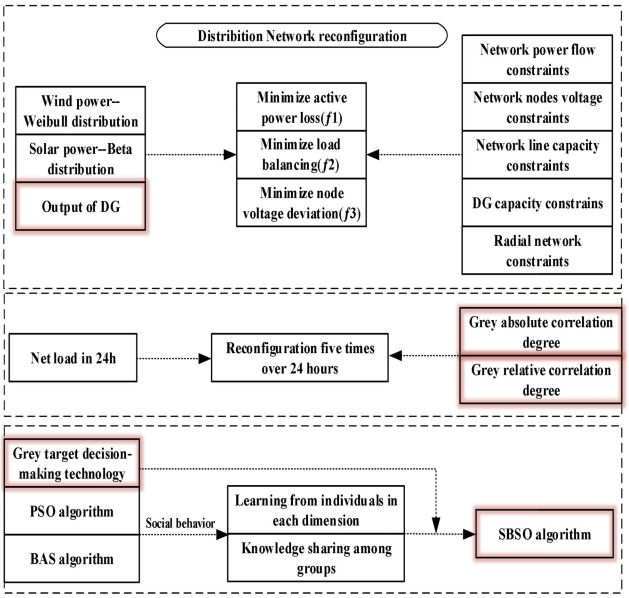

FIGURE 1. Outline of this paper.

3 SBSO algorithm combined GTDM is utilized to solve the multiobjective model. This method can automatically identify the best solution without losing objectivity.

The overall framework of this paper is shown in Fig.1.

Section II provides the random model of renewable sources and GRP is used to divide the reconfiguration period. Section III introduces the objective functions and constraints. Section IV describes the simplification and encoding of topology based on a basic loop. Section V explains the SBSO algorithm combined grey target decision-making and the test results of 5 benchmark functions from the SBSO algorithm. Section VI shows the test results from the IEEE-33 system and IEEE-69 system. Finally, Section VII presents the paper's conclusions.

II. PARTITION OF TIME INTERVALS BASED ON DG AND LOAD

A. RANDOM MODEL OF RENEWABLE SOURCES

1) MODEL OF WIND POWER

The output of wind turbine changes with wind speed, and it is expressed as:

$$P = \frac{1}{2}\rho v_w^3 s C_p \tag{1}$$

where P is the actual shaft power obtained by the fan in W; ρ is the air density in kg/m^3; v_w is the actual wind speed in m/s; s is the swept area of the wind turbine in m^2; and C_p is the wind energy utilization coefficient, with a maximum value of 0.593. From (1), the output of the fan is directly proportional to the wind speed.

The Weibull distribution is useful and simple, so the Weibull distribution is used to simulate the wind speed distribution with high randomness [11] in this paper, shown as:

$$fw\,(v) = \frac{k_c^t}{c^t}\left(\frac{v_w}{c^t}\right)^{k_c^t-1}\exp\left[-\left(\frac{v_w}{c^t}\right)^{k_c^t}\right] \tag{2}$$

where c^t is the Weibull scale parameter and k_c^t is the Weibull shape parameter.

The relationship between wind speed and wind turbine active power output P_W is as follows:

$$P_W = \begin{cases} 0, & v_w < v_{ci}, v_w \geq v_{co} \\ P_r \dfrac{v - v_{ci}}{v_r - v_{ci}}, & v_{ci} \leq v_w \leq v_r \\ P_r, & v_r \leq v_w \leq v_{co} \end{cases} \tag{3}$$

where P_r is the rated capacity of the wind turbine; P_W is the actual power of the wind turbine; v_{ci} is the cut-in speed of wind power; v_r is the rated speed of wind power; and v_{co} is the cut-out speed of wind power. According to reference [11], the probability function of wind power output is as follows:

$$\begin{cases} P(P_W = 0) = 1 - \exp(-(\frac{v_{ci}}{c^t})^{k_c^t})) + \exp(-(\frac{v_{co}}{c^t})^{k_c^t}) \\ P(P_W = P_r) = \exp(-(\frac{v_r}{c^t})^{k_c^t})) - \exp(-(\frac{v_{co}}{c^t})^{k_c^t}) \\ f\,(P_W) = \dfrac{k_c^t}{k_1 c^t}\left(\dfrac{P_W - k_2}{k_1 c^t}\right)^{k_c^t-1}\exp\left[-\left(\dfrac{P_W - k_2}{k_1 c^t}\right)^{k_c^t}\right], \quad else \end{cases} \tag{4}$$

where $k_1 = P_r/(v_r - v_{ci})$ and $k_2 = v_{ci}P_r/(v_{ci} - v_r)$.

The output reactive power Q_W is:

$$Q_W = P_W \times \sqrt{1 - \cos\theta^2}/\cos\theta \tag{5}$$

where $cos\theta$ is the power factor.

2) MODEL OF SOLAR POWER

Photovoltaic power generation depends on climate and weather, which is greatly affected by solar radiation factors [13]. The solar radiation can be fitted by the beta function, and its probability density function is as follows:

$$f\,(E) = \frac{\Gamma\left(\alpha_c^t + \beta_c^t\right)}{\Gamma\left(\alpha_c^t\right)\Gamma\left(\beta_c^t\right)}\left(\frac{E}{E_{\max}}\right)^{\alpha_c^t-1}\left(1 - \frac{E}{E_{\max}}\right)^{\beta_c^t-1} \tag{6}$$

where Γ is the gamma function, α_c^t and β_c^t are the shape parameters of the distribution functions, and E_{max} is the maximum value of solar radiation, where E_{max} is the maximumsolar radiation set as 1000 W/m^2 based on the analysis of sample data.

The relationship between the solar radiation and the active output power of photovoltaic power generation P_S is as follows:

$$P_S = \begin{cases} !\,P_S = \left(E^2/\left(E_{\max}\cdot E_f\right)\right), & 0 < E < E_f \\ P_S = \left(E/E_{\max}\right), & E \geq E_f \end{cases} \tag{7}$$

where E_f is the fixed-point set as 120 W/m^2.

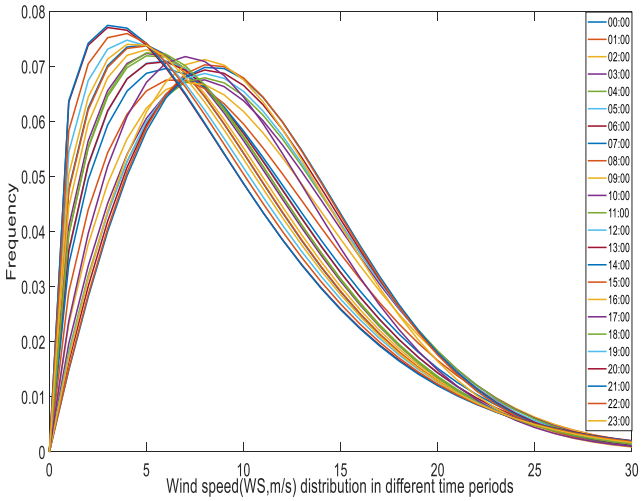

FIGURE 2. The PDF of wind speed in each period.

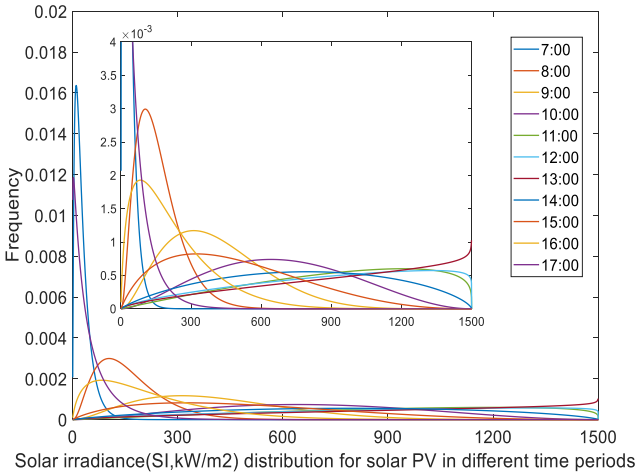

FIGURE 3. The PDF of solar irradiance in each period.

The probability density function of PV output in a specific area is:

$$f(P_S) = \begin{cases} \dfrac{1}{E_{\max}} \cdot \dfrac{\Gamma(\alpha_c^t + \beta_c^t)}{2 \cdot \Gamma\alpha_c^t \Gamma(\beta_c^t)} \left(\dfrac{P_S \cdot E_f}{P_{SR} E_{\max}}\right)^{\frac{\alpha_c^t - 1}{2}} \\ \times \left(1 - \left(\dfrac{P_S \cdot E_f}{P_{SR} \cdot E_{\max}}\right)^{\frac{1}{2}}\right)^{\beta_c^t - 1} \times \left(\dfrac{E_{\max} E_f}{P_S P_{SR}}\right)^{\frac{1}{2}}, \\ 0 < P_S < \dfrac{P_{SR} E_f}{E_{\max}} \\ \dfrac{1}{E_{\max}} \cdot \dfrac{\Gamma(\alpha_c^t + \beta_c^t)}{\Gamma(\alpha_c^t)\Gamma(\beta_c^t)} \left(\dfrac{P_S}{P_{SR}}\right)^{\alpha_c^t - 1} \\ \times \left(1 - \dfrac{P_S}{P_{SR}}\right)^{\beta_c^t - 1} \times \dfrac{E_{\max}}{P_{SR}}, \quad P_S \geq \dfrac{P_{SR} E_f}{E_{\max}} \end{cases} \tag{8}$$

where P_{SR} is the maximum output power of photovoltaic power generation

The cutoff wind speed $v_{ci} = 5$ m/s, the cut-out wind speed $v_{co} = 24$ m/s, and the rated wind speed $v_r = 11$ m/s. The wind speed at the height of the fan impeller hub in this area obeys the Weibull distribution of c^t and k_c^t and the solar radiation obeys the beta distribution of α_c^t and β_c^t, The parameters of c^t, k_c^t, α_c^t and β_c^t are obtained from 8760 samples of actual wind speed and actual solar radiation data in a region [35], as shown in Table 1.

The PDFs of Weibull and Beta distributions fitted to each hour are shown in Figs. 2 and 3.

The probability density distribution function of wind power and photovoltaic output is obtained by substituting the parameter c^t, k_c^t, α_c^t and β_c^t into the above equations to calculate the integral. Simpson formula is used to solve the problem to speed up the speed of solution, and the expected wind power and photovoltaic output is obtained as follows, they are shown in Figs.4 and 5.

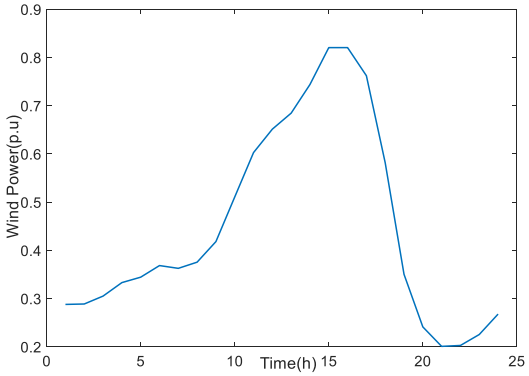

FIGURE 4. The expected output of wind power.

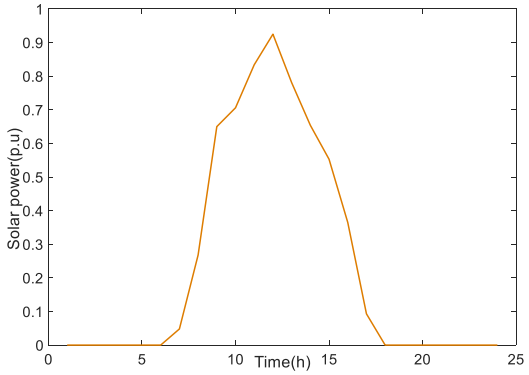

FIGURE 5. The expected output of solar power.

B. LOAD DEMAND

Users usually have relatively fixed demand proportion curves during a typical day in the same region and season, the loads can be described by demand proportion curves per day [36], which is shown in Fig.6.

In general, the daily loads involve three categories: residential, industrial and commercial, the concrete parameters are given in Tables 2 and 3, they are shown in Fig.7.

TABLE 1. The control parameters of Weibull and Beta in each period.

Time(h)	0	1	2	3	4	5	6	7	8	9	10	11
k_c	1.474	1.476	1.501	1.539	1.554	1.586	1.580	1.60	1.654	1.745	1.819	1.854
c	10.02	10.05	10.20	10.37	10.45	10.67	10.68	10.93	11.39	11.79	11.97	12.05
α_c	0	0	0	0	0	0	4.99	7.49	6.54	5.88	4.06	3.38
β_c	0	0	0	0	0	0	33.81	16.32	6.43	3.05	1.24	1.09
Time(h)	12	13	14	15	16	17	18	19	20	21	22	23
k_c	1.874	1.911	1.956	1.954	1.914	1.784	1.559	1.403	1.327	1.329	1.373	1.445
c	11.98	12.01	12.09	12.00	11.71	11.16	10.38	9.84	9.51	9.46	9.65	9.95
α_c	3.27	3.80	4.07	3.80	2.47	0	0	0	0	0	0	0
β_c	0.93	1.67	3.39	6.85	12.19	0	0	0	0	0	0	0

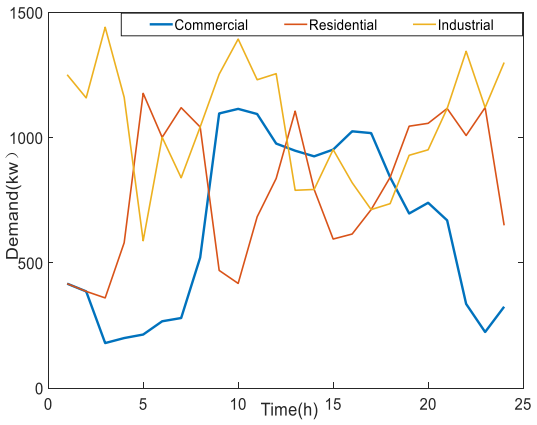

FIGURE 6. Load duration curves of each type for 24 hours.

TABLE 2. The load distribution in hours of three types of load.

Hours	Residential/Industrial/Commercial load			Hours	Residential/Industrial/Commercial load		
1	0.1	0.3	0.1	13	0.7	0.5	0.6
2	0.1	0.3	0.1	14	0.6	0.6	0.7
3	0.1	0.4	0	15	0.5	0.8	0.8
4	0.1	0.2	0	16	0.6	0.8	1
5	0.4	0.2	0	17	0.7	0.7	1
6	0.3	0.3	0	18	0.8	0.7	0.8
7	0.4	0.3	0.1	19	0.9	0.8	0.6
8	0.4	0.4	0.2	20	1	0.9	0.7
9	0.3	0.8	0.7	21	1	1	0.6
10	0.3	1	0.8	22	0.6	0.8	0.2
11	0.5	0.9	0.8	23	0.5	0.5	0.1
12	0.6	0.9	0.7	24	0.2	0.4	0.1

The load curves of each node are different, and the daily load curve P_{Li} of node 'i' can be described as:

$$P_{Li} = \sum_{s \in S} P_{Ni}\theta_{si}\delta_s \tag{9}$$

where $S \in \{s|1, 2, 3\}$ is the set of load types; $s = 1$ is residential, $s = 2$ is industrial, and $s = 3$ is commercial; P_{Ni} is the rated power of load node 'i'; and θ_{si} represents the ratio of load type 's' in the total load of node 'i', δ_s represents the demand curves of load type 's' [36].

TABLE 3. The proportion of three types of load in each bus.

Nodes	Residential/Industrial/Commercial load			Nodes	Residential/Industrial/Commercial load		
2	0.5	0.3	0.2	18	0.5	0.1	0.4
3	0.3	0.2	0.5	19	0.2	0.3	0.5
4	0.2	0.3	0.5	20	0.3	0	0.7
5	0.1	0.3	0.6	21	0.3	0.2	0.5
6	0.4	0.2	0.4	22	0	0.7	0.3
7	0	0.4	0.6	23	0.4	0.1	0.5
8	0.3	0.4	0.3	24	0.5	0.1	0.4
9	0.6	0	0.4	25	0.4	0	0.6
10	0	0.7	0.3	26	0.3	0	0.7
11	0.2	0.2	0.6	27	0	0.9	0.1
12	0.5	0	0.5	28	0.3	0.1	0.6
13	0.4	0	0.6	29	0.1	0.5	0.4
14	0.4	0.2	0.4	30	0.2	0.1	0.7
15	0.1	0.4	0.5	31	0.4	0.2	0.4
16	0.7	0.1	0.2	32	0.1	0.7	0.2
17	0.3	0.4	0.3	33	0.7	0	0.3

TABLE 4. Type, location and capacity of DG.

Type	Location	Capacity/kW	Power factor
Wind turbine	10	400	0.95
Wind turbine	33	500	0.95
photovoltaic panels	7	350	0.95
photovoltaic panels	14	450	0.95

C. NET LOAD

Parameters of DG type, capacity and access node are shown in Table 4 [37].

According to the above analysis, the net load on each node is obtained.

$$P_{NLi} = P_{Li} - P_{Wi} - P_{Si} \tag{10}$$

D. PARTITION OF TIME INTERVALS BASED ON GREY RELATION PROJECTION ANALYSIS

The combination of unit periods with similar network properties can greatly reduce the number of switching operations in the process of distribution network reconfiguration, and GRP is an effective method to analyze the similarity of sample data. Through the analysis of small sample data to judge whether different data series are closely related, the closer

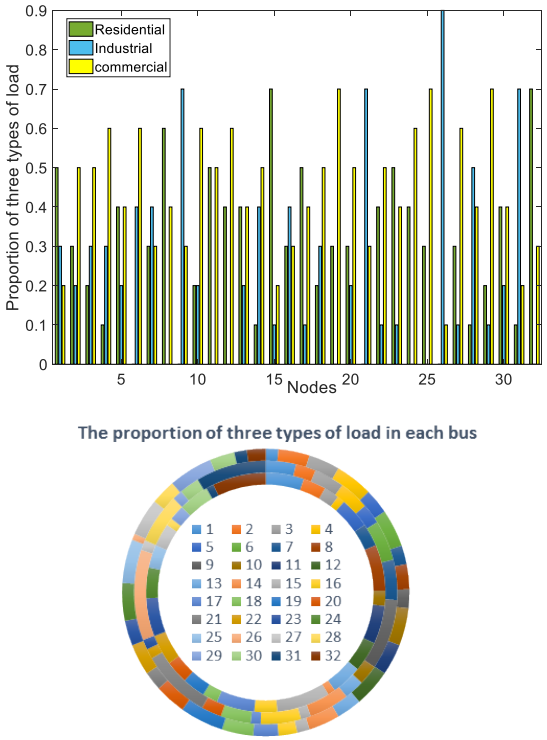

FIGURE 7. The proportion of three types of load in each bus.

the sequence is, the greater the correlation degree is, so the effective data sequence was clustered.

The sample data needed is small and the calculation is simple while using the grey correlation analysis and clustering. At the same time, this method can effectively reduce the number of switching operations, which is more economical.

Taking the net load on different nodes as a group of sample data, the grey correlation analysis is utilized to analyse the similarity of sample data.

$Xt = (xt(1), xt(2), \ldots, xt(i), \ldots, xt(n))$, $(t = 1, 2, \ldots, 24, i = 1, 2, \ldots, 33)$ is the sample data.

The original sequence is multiplied by the starting point zero operator D^0 in order to be analyzed by grey absolute correlation analysis.

$$X_t D^0 = (x_t(1)d^0, x_t(2)d^0, \ldots, x_t(i)d^0, \ldots, x_t(n)d^0),$$
$$X_t^0(i) = x_t(i)d^0 = x_t(i) - x_t(1).$$

Grey absolute correlation degree $\varepsilon_{t,t+1}$ is obtained by equations (11)-(13).

$$\varepsilon_{t,t+1} = \frac{1 + \left|S_t^0\right| + \left|S_{t+1}^0\right|}{1 + \left|S_t^0\right| + \left|S_{t+1}^0\right| + \left|S_{t+1}^0 - S_t^0\right|} \tag{11}$$

$$\left|S_t^0\right| = \left|\sum_{i=2}^{n-1} x_t^0(i) + \frac{1}{2}x_t^0(n)\right| \tag{12}$$

$$\left|S_{t+1}^0 - S_t^0\right| = \left|\sum_{i=2}^{n-1}\left(x_{t+1}^0(i) - x_t^0(i)\right) + \frac{1}{2}\left(x_{t+1}^0(n) - x_t^0(n)\right)\right| \tag{13}$$

The original sequence is multiplied by the initial valued operator D^1 in order to be analyzed by grey absolute correlation analysis.

$$X_t D^1 = (x_t(1)d^1, x_t(2)d^1, \ldots, x_t(i)d^1, \ldots, x_t(n)d^1),$$
$$x_t(i)d^1 = x_t(i)/x_t(1).$$

Grey relative correlation degree $r_{t,t+1}$ is obtained by equations (14)-(16).

$$r_{t,t+1} = \frac{1 + \left|S_t^1\right| + \left|S_{t+1}^1\right|}{1 + \left|S_t^1\right| + \left|S_{t+1}^1\right| + \left|S_{t+1}^1 - S_t^1\right|} \tag{14}$$

$$\left|S_t^1\right| = \left|\sum_{i=2}^{n-1} x_t^1(i) + \frac{1}{2}x_t^1(n)\right| \tag{15}$$

$$\left|S_{t+1}^1 - S_t^1\right| = \left|\sum_{i=2}^{n-1}\left(x_{t+1}^1(i) - x_t^1(i)\right) + \frac{1}{2}\left(x_{t+1}^1(n) - x_t^1(n)\right)\right| \tag{16}$$

The grey comprehensive correlation degree not only represents the similarity degree of sequences X_t and X_{t+1}, but also reflects the similarity degree of change rate relative to the starting point. It can comprehensively reflect whether the connection between sequences is close, the grey comprehensive correlation degree is obtained.

$$\rho_{t,t+1} = \theta\varepsilon_{t,t+1} + (1 - \theta)\, r_{t,t+1}, \quad \theta \in [0, 1] \tag{17}$$

In the actual process of reconfiguration, we pay more attention to the similarity of the sequence. The more similar the net load distribution on the nodes, the better the unit period consolidation can be combined. When the absolute correlation degree is more important, the absolute correlation degree is given greater weight. In this paper, we take $\theta = 0.7$.

III. MULTIOBJECTIVE MODEL OF DISTRIBUTION NETWORK RECONFIGURATION

A. MULTIOBJECTIVE MODEL

In this paper, aiming at minimizing active power loss, load balancing and the maximum voltage deviation, a multiobjective model of the distribution network is formed.

The minimization of the sum of active power loss is:

$$f^{(1)} = \min \sum_{t=1}^{T}\sum_{j}^{J} D_j R_j \frac{P_j^2 + Q_j^2}{V_j^2} \tag{18}$$

where P_j is the active power of the *j-th* branch, Q_j is the reactive power of the *j-th* branch, R_j is the resistance of the *j-th* branch, V_j is the initial voltage of the *j-th* branch, and D_j is the binary value. If D_j is the opening switch status for the *j-th* branch, $D_j = 0$; otherwise, $D_j = 1$. J is the number of branches, and T is the time length.

The minimization of the sum of load balancing is:

$$f^{(2)} = \min \sum_{t=1}^{T}\sum_{j=1}^{J} D_j \frac{\sqrt{P_j^2 + Q_j^2}}{S_j^{\max}} \tag{19}$$

where S_j^{max} is the maximum complex power of branch 'j'.

The minimization of the sum of maximum voltage deviation is:

$$f^{(3)} = \min\left(\sum_{t=1}^{T} \max\left(\frac{V_1 - V_{1r}}{V_{1r}}, \ldots, \frac{V_n - V_{nr}}{V_n}, \ldots, \frac{V_N - V_{Nr}}{V_{Nr}}\right)\right) \tag{20}$$

where V_n is the virtual voltage of the n-th node, V_{nr} is the rated voltage of the nth node, and N is the total number of nodes.

B. CONSTRAINTS

The following constraints must be meet in DNRC.

a: POWER FLOW EQUATION CONSTRAINTS

$$\begin{aligned} P_n + P_{DG,n} &= P_{L,n} + U_n \sum_{q=1}^{N} U_q \left(G_{nq}\cos\theta_{nq} + B_{nq}\sin\theta_{nq}\right) \\ Q_n + Q_{DG,n} &= Q_{L,n} + U_n \sum_{q=1}^{N} U_q \left(G_{nq}\sin\theta_{nq} - B_{nq}\cos\theta_{nq}\right) \end{aligned} \tag{21}$$

where P_n and Q_n are the active and reactive power injected on node n, respectively; $P_{DG,n}$, $Q_{DG,n}$ are the active and reactive power output of DG on node n, respectively; $P_{L,n}$ and $Q_{L,n}$ are the active and reactive power of the load on node n, respectively; G_{nq}, B_{nq}, θ_{nq} are the conductance, susceptance, and voltage phase angle difference of the branch between nodes n and q, respectively; U_n and U_q are the voltages of nodes n and q, respectively; and N is the number of system nodes.

b: NODE VOLTAGE CONSTRAINTS

$$U_{n,\min} \le U_n \le U_{n,\max} \quad (n = 1, \ldots, N) \tag{22}$$

$U_{n,min}$ and $U_{n,max}$ are the lower and upper voltage limits of node n, respectively.

c: BRANCH POWER CONSTRAINTS

$$S_j \le S_{j,\max} \quad (j = 1, \ldots, J) \tag{23}$$

S_j is the power of branch j; $S_{j,max}$ is the maximum power allowed by branch j, and J is the total number of branches.

d: DG CAPACITY CONSTRAINTS

$$P_{DG,n,\min} \le P_{DG,n} \le P_{DG,n,\max} \quad (n = 1, \ldots, N_{DG}) \tag{24}$$

$P_{DG,n}$ is the active output of distributed energy on node n; $P_{DG,n,min}$, $P_{DG,n,max}$ are the minimum and maximum output power of distributed energy on node n, respectively; and N_{DG} is the total number of distributed generations.

e: NETWORK CONSTRAINTS

The distribution network cannot appear loops and islands, it must be radial.

When the constraint condition exceeds the limit, it is included in the penalty function, the amount of the limit determines the size of the penalty, and finally, the penalty function is included in the objective function [38].

IV. NETWORK SIMPLIFIED CODING

In this paper, the IEEE-33 node system with DG is selected. 33 nodes, 32 section switches and 5 tie switches appear in this system. And the reference voltage is 12.66 kV. The specific parameters are shown in [39].

The DG type, capacity and access node are shown in Table. 4.

There are many switches in the DNRC, so the particle dimension is large. To avoid many infeasible solutions, the coding strategy of the distribution network is shown in Table. 5.

The distribution network in this paper is divided into five ring networks by the coding strategy in reference [40]. In each ring network, only one switch is able to be disconnected, which ensures the radial topology of the distribution network and the infeasible solutions are largely excluded.

The network loop switch matrix is defined as:

$$SL_{su} = \left(a_{a,b}\right)_{w\times w} \tag{25}$$

where w is the number of interconnection switches; SL_{su} is a 0/1 matrix; and if the switch number b corresponding switch is in loop a, $a_{a,b}$ is 1; otherwise, it is 0. For example, the numbered particle S_{su} = [3 6 11 12 2] corresponds to switches (4, 14, 4, 17, 4). Switch 4 is in loop 1, so $\alpha_{1,1}$ is 1; switch 14 is not in loop 1, so $\alpha_{1,2}$ is 0; switch 4 is in loop 1, so $\alpha_{1,3}$ is 1; switch 17 is not in loop 1, so $\alpha_{1,4}$ is 0; switch 4 is in loop 1, so $\alpha_{1,5}$ is 1; and so on, the corresponding SL_{su} is:

$$SL_{su} = \begin{bmatrix} 1 & 0 & 1 & 0 & 1 \\ 0 & 1 & 0 & 0 & 0 \\ 1 & 0 & 1 & 0 & 1 \\ 0 & 0 & 0 & 1 & 0 \\ 1 & 0 & 1 & 0 & 1 \end{bmatrix} \tag{26}$$

The SL_{su} matrix corresponding to S_{su} is a nondiagonal matrix, if the same row appears in the matrix, it indicates that the public switch in the loop has been turned on not only one time, and the loop network appears in the network, which is an infeasible solution. If the elements of a row of SL_{su} are all 0, there are no switch turned on in the ring network, which indicates that an island has been generated, and the particle is also an infeasible solution.

In summary, $R\,(SL_{su})$ is the rank R of SL_{su}; if $R(SL_{su}) < a$, the particle is an infeasible solution.

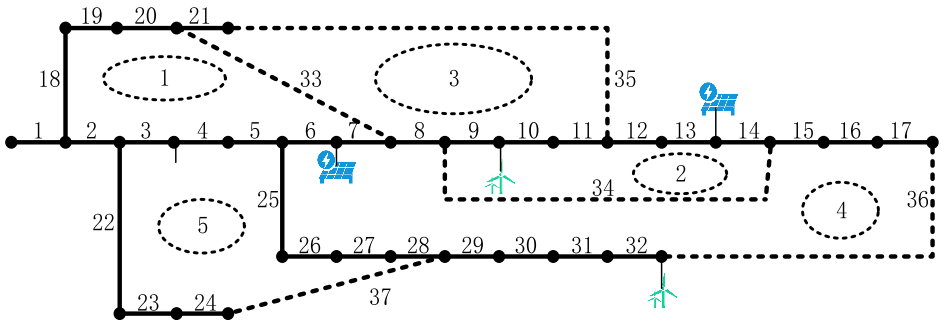

FIGURE 8. Simplified diagram of the IEEE 33-bus distribution network.

TABLE 5. Loop vectors of the IEEE 33-bus distribution network.

Loop	interconnection switch	number in a loop	number of switches
1	33	1-10	2,3,4,5,6,7,20,19,18,33
2	34	1-7	9,10,11,12,13,14,34
3	35	1-15	8,9,10,11,21,20,19,18,2,3,4,5,6,7,35
4	36	1-21	6,7,8,9,10,11,12,13,14,15,16,17,32,31,30,29,28,27,26,25,36
5	37	1-11	3,4,5,25,26,27,28,24,23,22,37

V. IMPROVED SBSO ALGORITHM BASED ON GREY TARGET DECISION-MAKING

A. IMPROVED SBSO ALGORITHM

X. Jiang first proposed the beetle antennae search algorithm in 2017. The beetle moves by comparing the fitness values corresponding to the two antenna positions of the beetle. If the left fitness value of the beetle is greater than that of the right, the beetle moves to the left, vice versa [32], [33]. In this paper, multidimensional function optimization is taken as an example to solve the optimal value. The steps are as follows:

(1) The position of the beetle in the o-dimensional solution space is:

$$X^0 = (x_1, x_2, \ldots, x_o) \tag{27}$$

(2) The spatial coordinates of the left and right sides of beetles are as follows:

$$\begin{cases} x_l = x + L\vec{b} \\ x_r = x - L\vec{b} \end{cases} \tag{28}$$

where x_l is the left side of the search area, x_r is the right side of the search area, which is a random unit vector, L is the distance from two whiskers to the center of mass, and $\vec{b}$ is the random unit vector.

(3) The update rule of beetle is as follows:

$$x^{t+1} = x^t - \delta^t \cdot \vec{b} \cdot sign\left[f\left(x_l^t\right) - f\left(x_r^t\right)\right] \tag{29}$$

where x^t is the centroid coordinates of the *t-th* iteration of the beetle; x_l^t and x_r^t are the left and right antennas of the *t-th* iteration, respectively; $f(x)$ is the fitness value of x; δ^t is the step size at the *t-th* iteration; and *sign(x)* is a sign function.

The BAS algorithm only focuses on the individual, the PSO algorithm is for groups. So, to improve the performance of optimization algorithm, the BAS algorithm and PSO algorithm are combined in this paper [41], [42], and reduce the computational time by social behaviors between beetles.

To avoid premature convergence, the SBSO algorithm considering chaos migration strategy is used in this paper.

The similarity of beetles is:

$$S = \sum_{p=1}^{NP} s_p \tag{30}$$

$$s_p = \begin{cases} 1, & d(q,p) < \dfrac{d_{\max} - d_{\min}}{2} \\ 0, & d(q,p) \geq \dfrac{d_{\max} - d_{\min}}{2} \end{cases} \tag{31}$$

where *d(q,p)* is the Euclidean distance from individual q to p, q is the beetle with the best fitness value, d_{min} is the Euclidean distance of the nearest individual to q, and d_{max} is the Euclidean distance of the beetle farthest from q, B is the number of populations.

The logistic map is:

$$\begin{cases} X_d = \eta X_d^s \left(1 - X_d^s\right), & S > 0.2B \\ No\ chaotic\ disturbance, & if\ not \end{cases} \tag{32}$$

where X_d is the d-dimensional variable of chaotic sequence X, $X_d \in [0; 1]$, and $\eta \in (3.569, 4)$.

The chaos initial population is scaled into [0, 1], and the chaotic sequence $G = \{X^1 \ldots, X^S\}$ is obtained iteratively.

$$newX_d = b_{\min} + (b_{\max} - b_{\min}) X_d$$

where b_{max} and b_{min} are the upper and lower boundary values of the d-dimensional variable new X_d, respectively.

The iterative process from t to $t+1$ for individual p is:

$$x_{pd}^{t+1} = \begin{cases} round\left(x_{pd}^t + Y^t + V^{t+1}\right), & if\ p_p^t > P_p^L \\ x_{pd}^t, & otherwise \end{cases} \tag{33}$$

where P_p^L is the learning probability of individual p, which is inversely proportional to its own fitness value; p_p^t is the random number of individual p, with a value of [0, 1].

In the SBSO algorithm, the cognitive factors and social learning factors are considered. And, the bad particles are replaced by the preference random method in each iteration, the particles with bad fitness values are eliminated during this progress. Based on this, an improved beetle search particle swarm optimization algorithm was proposed.

In the knowledge sharing process, beetles can obtain the information from individuals who are better than themselves and learn the knowledge from the average status of the social group including bad beetles to handle the problem of premature convergence, the social learning factors are proposed considering these two social behaviors [43]–[45]. Beetles can learn from different individuals in each dimension, which can greatly reduce the number of iterations and solve high-dimensional and complex problems.

Thus, the speed update rules of the beetle are as follows:

$$\left.\begin{aligned} Y^t &= z_0^t \vec{b} sign\left(f\left(x_r^t\right) - f\left(x_l^t\right)\right) \\ V^{t+1} &= z_1 V^t + z_2\left(x_{pd}^t - x_{bd}^t\right) + z_3\varepsilon\left(x_{pd}^t - x_m^t\right) \\ z_1 &= z_{1,\max} - \frac{\left(z_{1,\max} - z_{1,\min}\right)\cdot t}{T_{\max}} \\ x_m^t &= \frac{\left(x_{pd}^t - x_{\min,d}^t\right)\left(x_{\max,d}^t - x_{\min,d}^t\right)}{x_{pd}^t - x_{\max,d}^t} + x_{\min,d}^t \end{aligned}\right\} \tag{34}$$

where $b(P_b > P_p)$ is the individual randomly selected by individual p among populations with greater fitness than that of itself, and individual p can learn from different objects randomly in different dimensions. p can learn from different objects who are better than it, which can obtain more useful information during this process. x_{pd}^t is the position of the individual p in the d dimension of generation $t(1 \le d \le D)$; D is the dimension of the decision space; z_0^t is a cognitive factor; $z_2 - z_3$ are random numbers of individual p between [0, 1]; ε is the influence factor for controlling the social influence of x_m^t, which is taken as 0.01 in this paper; $z_{1,max}, z_{1,min}$ are the maximum and minimum inertia weights, respectively; T_{max} is the maximum number of iterations; and $x_{max,d}^t, x_{min,d}^t$ are the upper and lower search bounds of the d-dimension variables, respectively.

When the individual is lower than the average value, the individual performance is not good. So, to strengthen the global search ability, it is necessary to increase the cognitive factor; otherwise, to accelerate the convergence speed, the cognitive factor is reduced [46].

$$\begin{cases} z_0^t = z_{0,\max} - \dfrac{\left(z_{0,\max} - z_{0,\min}\right)\left(F - F_{\min}^t\right)}{F_{\max}^t - F_{avg}^t}, & F \ge F_{avg}^t \\ z_0^t = z_{0,\max}, & F < F_{avg}^t \end{cases} \tag{35}$$

F, F_{min}, F_{max} and F_{avg} are the current individual fitness value, population minimum fitness value, population maximum fitness and average fitness, respectively; and $z_{0,max}$ and $z_{0,min}$ are the maximum and minimum cognitive factors, respectively.

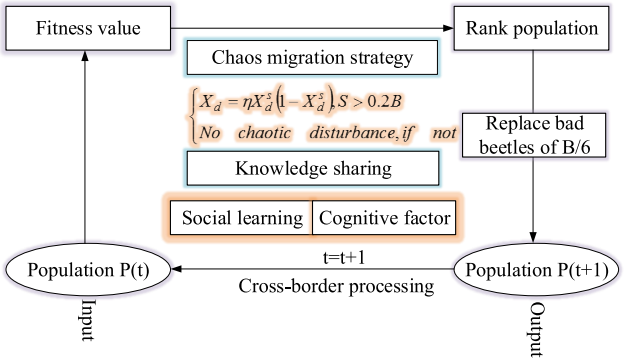

FIGURE 9. Chaos migration strategy and social learning strategy.

Rank the fitness values and replace the last beetles of *B/6*. In order to make full use of the effective information of the current solution set, the preference random method is used to update the position of the beetle to reduce the probability of falling into the local optimal solution.

Replace the bad beetles by the following formula:

$$x_{pr}^{t+1} = x_{pr}^t + z_4\left(x_{p,1}^t - x_{p,2}^t\right) \tag{36}$$

x_{pr}^t is the bad beetle; $x_{p,1}^t$ and $x_{p,2}^t$ are any two different particles in the population; and z_4 is random numbers of individual p between [0, 1].

The probability function is:

$$P_p^L = 1 - \frac{g-1}{B} \tag{37}$$

where g is the rank of individual p in the population after fitness sorting.

The chaos migration strategy and the social learning strategy are shown in Fig. 9.

B. GREY TARGET DECISION-MAKING

GTDM is one of the useful methods to solve multi-index decision-making problems in grey system theory, which can be used to optimize the optimal solution. GTDM is to measure and transform all indexes to the Euclidean space of the same dimension, that is, grey target. A target center is found in the grey target as the standard model, and then the decision points in the grey target are compared with the target center, and different target center distances are obtained to obtain the optimal scheme. The weight and target distance of each scheme are calculated based on entropy value, which does not depend on expert evaluation or decision-maker's preference, so as to improve the credibility and authenticity of decision-making. In this paper, the GTDM is used to analyze and solve the multiobjective distribution network reconfiguration, so that the sum of the active power loss, the load balancing index, and the maximum node voltage deviation index can simultaneously reach the optimal.

The four elements of grey decision-making are event, strategy, target and effect.

Distribution network reconfiguration event is $A = \{a_1\}$, and all possible strategy set are $B = \{b_1, b_2, \ldots, b_B\}$, in which $b_p(p = 1, 2, \ldots, B)$ is the *p-strategy*.

The decision scheme set S of grey decision is the Cartesian product of event set $A = \{a_1\}$ and strategy set $B = \{b_1, b_2, \ldots, b_B\}$.

$$\begin{aligned} S = A \times B &= \left\{ \left(a_1, b_p\right) \middle| a_1 \in A, b_p \in B \right\} \\ &= \{s_{11}, s_{12}, \ldots, s_{1B}\} \end{aligned} \tag{38}$$

The decision scheme set S is obtained by SBSO algorithm, that is the break switch combination of the *p-th* beetle.

The objective of GTDM is the goal of distribution network reconfiguration $f^{(k)}(k = 1, 2, 3)$. At the same time, $u_{1p}^{(k)}$ is the effect value of the decision scheme set S_{1p} of objective k.

$$u_{1p}^{(k)} : S \mapsto R, S_{1p} \mapsto u_{1p}^{(k)} \tag{39}$$

$u_{1p}^{(k)}$ is the effect mapping of S with respect to objective 'k' and represents the satisfaction degree of *p-decision-making* under *k-objective*.

$$u_{1p}^{(k)} = \lambda_1 f_{1p}^{k} + \lambda_2 f_S \tag{40}$$

where $f_{1p}^{(k)}$ is the evaluation index of scheme S_{1p} with respect to objective 'k', f_S is the number of switching operation index. λ_1 and λ_2 is calculated by the entropy method.

fs is modeled as follows:

$$f_S = \sum_{t}^{T} \sum_{m}^{M} 0.5(D_{m,p+1} \oplus D_{m,p} + D_{m,p} \oplus D_{m,p-1}) \tag{41}$$

where $D_{m,p}$ is the status of switch 'm' of reconguration scheme S_{1p}, $D_{m,p+1}$ and $D_{m,p-1}$ are the statuses of switch 'm' for the other two reconfiguration schemes.

Since the meaning, dimension and properties of different target effect values is different, in order to obtain a comparable comprehensive effect measure, the target effect value $u_{1p}^{(k)}$ is transformed into a consistent effect measure $r_{1p}^{(k)}$ based on the averaging operator $t^{(k)}$.

$$t^{(k)} = \frac{1}{B} \sum_{p=1}^{B} u_{1p}^{(k)}, \quad k = 1, 2, \ldots, K \tag{42}$$

If the target value is benefit index,

$$r_{1p}^{(k)} = \frac{\left(u_{1p}^{(k)} - t^{(k)}\right)}{\max\left\{ \max\limits_{1 \le p \le B} \left\{u_{1p}^{(k)}\right\} - t^{(k)}, t^{(k)} - \min\limits_{1 \le p \le B} \left\{u_{1p}^{(k)}\right\} \right\}} \tag{43}$$

If the target value is a cost index,

$$r_{1p}^{(k)} = \frac{\left(t^{(k)} - u_{1p}^{(k)}\right)}{\max\left\{ \max\limits_{1 \le p \le B} \left\{u_{1p}^{(k)}\right\} - t^{(k)}, t^{(k)} - \min\limits_{1 \le p \le B} \left\{u_{1p}^{(k)}\right\} \right\}} \tag{44}$$

If the target value is an interval index of [a, b],

$$r_{1p}^{(k)} = \begin{cases} \dfrac{2u_{1p}^{(k)} - a - \min\limits_{1 \le p \le B} \left\{u_{1p}^{(k)}\right\}}{a - \min\limits_{1 \le p \le B} \left\{u_{1p}^{(k)}\right\}}, & u_{1p}^{(k)} < a \\ 1, a \le u_{1p}^{(k)} \le b \\ -\dfrac{2u_{1p}^{(k)} - b - \max\limits_{1 \le p \le B} \left\{u_{1p}^{(k)}\right\}}{\max\limits_{1 \le p \le B} \left\{u_{1p}^{(k)}\right\} - b}, & u_{1p}^{(k)} > b \end{cases} \tag{45}$$

Based on the above transformation, the consistent effect matrix $R^{(k)}$ is obtained.

$$R^{(k)} = \left(r_{1p}^{(k)}\right) = \begin{bmatrix} r_{11}^{(k)} & r_{12}^{(k)} & \ldots & r_{1B}^{(k)} \end{bmatrix} \tag{46}$$

There is only one event a_1 in the grey decision model of distribution network reconfiguration, and its consistent effect matrix can be transformed into a decision matrix R corresponding to objectives and strategies.

$$R = \left(r_{kp}\right)_{K \times B}, \left(r_{kp} = r_{1p}^{(k)}\right) \textit{ and } \left(r_{kp} \in [-1, 1]\right) \tag{47}$$

Finally, the center of GTDM R^0 is determined.

$$R^0 = \begin{bmatrix} R_1^0 & \ldots & R_k^0 & \ldots & R_K^0 \end{bmatrix} \tag{48}$$

R^0 is described as follows:

$$R_k^0 = \max\left\{ r_{kp} \middle| 1 \le p \le B \right\} \tag{49}$$

The target distance reflects the advantages and disadvantages of each scheme. The smaller the target distance is, the closer the scheme is to the ideal one, the better the scheme is, and vice versa. Therefore, the scheme with the minimum target distance is the optimal one [30].

Effect vector R_p of scheme p is described as follows:

$$R_p = \begin{bmatrix} R_{1p} & \ldots & R_{kp} & \ldots & R_{Kp} \end{bmatrix} \tag{50}$$

Target distance d_p of scheme p is described as follows:

$$d_p = \left| R_p - R^0 \right| = \sqrt{\sum_{k=1}^{K} \phi_k \left(R_{kp} - R_k^0\right)^2} \tag{51}$$

where φ_k ($\varphi_k(k = 1, 2, \ldots, K)$ is the weight of each target.

The weight coefficient reflects the influence of objective k on decision-making.

In this study, the weights are obtained by the comprehensive analytic hierarchy process (AHP) and entropy weight method [30], [47]. Firstly, the static weight is calculated by AHP, and then the improved weight is determined by the entropy weight method, and is used to modify the static weight to obtain the comprehensive weight φ_k.

1) AHP is used to determine the static weight, the importance of K parameters is assigned and then the judgment

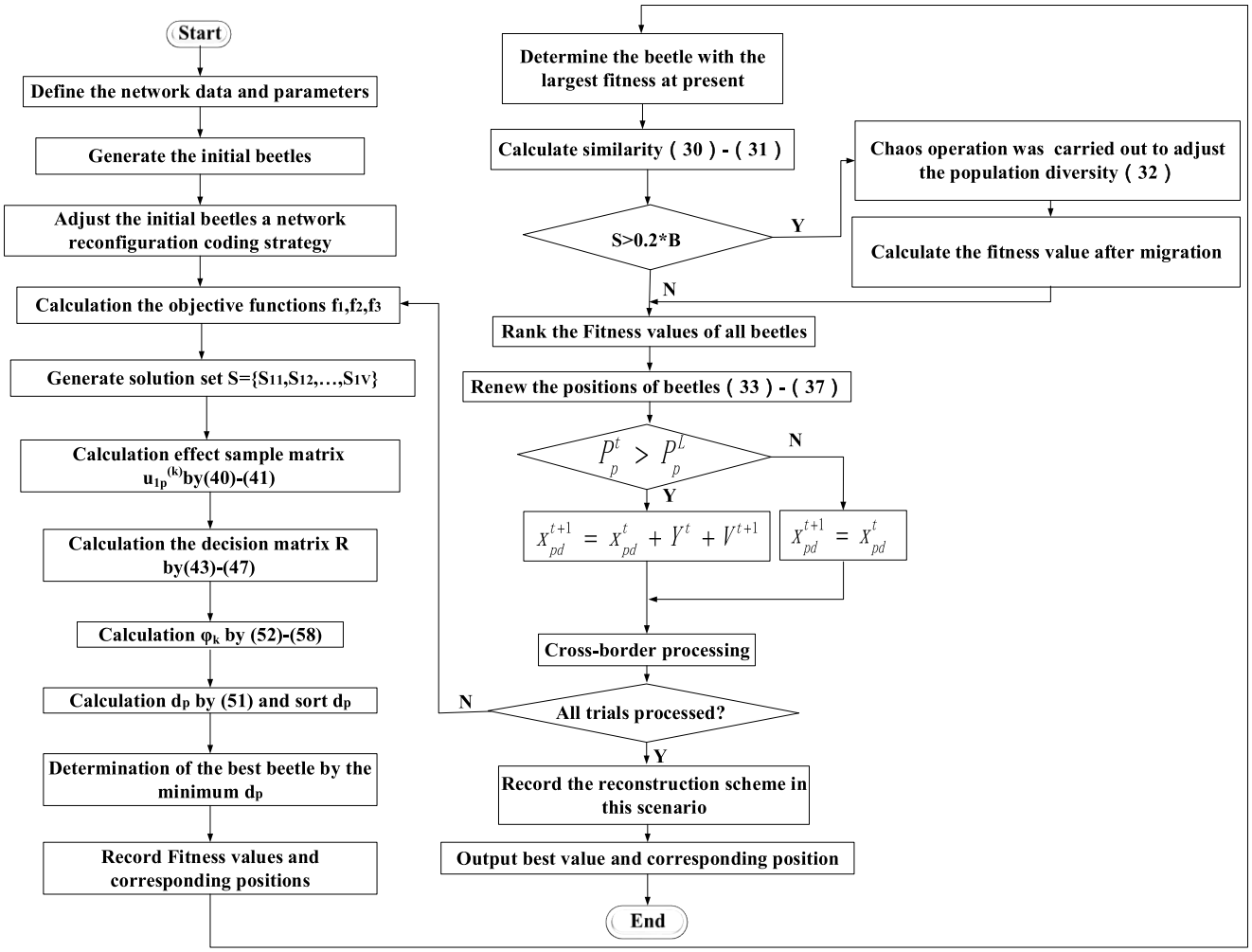

FIGURE 10. The algorithm flow chart of this paper.

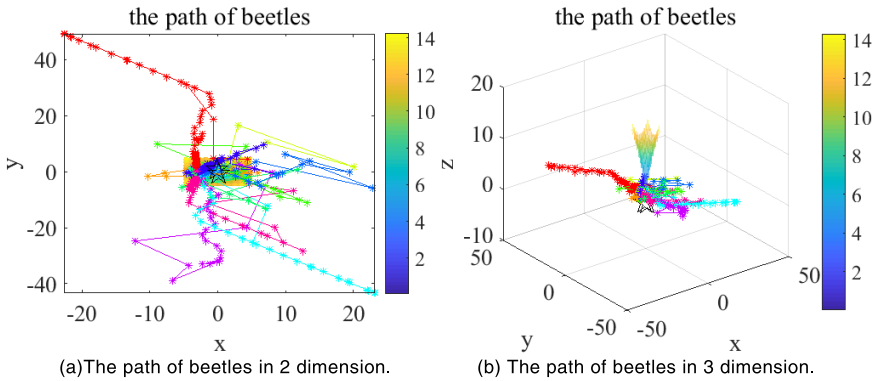

(a)The path of beetles in 2 dimension. (b) The path of beetles in 3 dimension.

FIGURE 11. The path of beetles.

matrix is obtained according to the results of comparison.

$$I = \begin{bmatrix} \frac{\alpha_1}{\alpha_1} & \frac{\alpha_1}{\alpha_2} & \cdots & \frac{\alpha_1}{\alpha_K} \\ \frac{\alpha_2}{\alpha_1} & \frac{\alpha_2}{\alpha_2} & \cdots & \frac{\alpha_2}{\alpha_K} \\ \cdots & \cdots & \cdots & \cdots \\ \frac{\alpha_K}{\alpha_1} & \frac{\alpha_K}{\alpha_2} & \cdots & \frac{\alpha_K}{\alpha_K} \end{bmatrix} \tag{52}$$

α_i/α_j is the importance of the *i-th* parameter relative to the *j* parameter. Then, the matrix weight method is used to find an optimal weight vector W for the judgment matrix A satisfying the consistency test condition.

$$W = (\beta_1, \beta_2, \ldots, \beta_K)^T \tag{53}$$

2) Entropy weight method is used to determine the improved weight, for the multiobjective evaluation problem

TABLE 6. Function expression.

F	Name	Function	Range	Fmin
F1	Arkley	$-20\exp\left(-0.2\sqrt{\frac{1}{D}\sum_{i=1}^{D}X_i^2}\right)-\exp\left[\frac{1}{D}\sum_{i=1}^{D}\cos(2\pi X_i)\right]+20+e$	$[-50,50]^D$	0
F2	Bohachevsky	$\sum_{i=1}^{D-1}\left[X_i^2+2X_{i+1}^2-0.3\cos(3\pi X_i)-0.4\cos(4\pi X_{i+1})+0.7\right]$	$[-50,50]^D$	0
F3	Rastrigrin	$\sum_{i=1}^{D}\left[X_i^2-\cos(2\pi X_i)+10\right]$	$[-10,10]^D$	0
F4	Griewank	$\frac{1}{4000}\sum_{i=1}^{D}X_i^2-\prod_{i=1}^{D}\cos\frac{X_i}{\sqrt{i}}+1$	$[-10,10]^D$	0
F5	Dixon_price	$(x_1-1)^2+\sum_{i=2}^{D}i\left(2x_i^2-x_{i-1}\right)^2$	$[-10,10]^D$	0

TABLE 7. Performance comparison of five functions.

F	Algorithm	First quartile	Third quartile	Average fitness	Mean iterations	Running time (s)
F1	PSO in [34]	2.0154	5.43216	3.24597	178	115.24
	BAS in [32]	4.66234	6.23432	4.82074	198	176.74
	BSO	0.3465	2.3172	0.45433	115	93.64
	SBSO	2.1158e-09	1.6464	0.00129	98	54.38
F2	PSO in [34]	2.5564	135.54	19.6456	189	165.87
	BAS in [32]	3.5489	594.68	234.984	205	177.64
	BSO	3.6456	89.466	4.64688	141	114.37
	SBSO	0.6444	2.9884	1.57934	113	87.85
F3	PSO in [34]	0.0325	0.5334	0.37746	165	114.64
	BAS in [32]	1.6456	6.4952	2.59484	171	133.85
	BSO	1.6916e-04	5.6465	0.68796	104	82.76
	SBSO	7.11e-15	3.9798	0.09446	78	54.49
F4	PSO in [34]	0.0643	0.9561	0.09542	245	204.18
	BAS in [32]	0.5469	12.645	0.85671	264	254.27
	BSO	0.0246	1.9462	0.04563	198	163.83
	SBSO	0.0099	0.2663	0.00985	165	135.44
F5	PSO in [34]	0.18953	21.5664	0.34896	198	174.75
	BAS in [32]	0.26595	43.29544	0.84564	176	135.67
	BSO	0.01956	19.19858	0.05394	127	87.34

with K parameters and B evaluation objects, the grey target coefficient matrix is described as follows:

$$Q=(\gamma_{ij})=\begin{bmatrix}\gamma_{11} & \gamma_{12} & \cdots & \gamma_{1K}\\ \gamma_{21} & \gamma_{22} & \cdots & \gamma_{2K}\\ \cdots & \cdots & \cdots & \cdots\\ \gamma_{B1} & \gamma_{B2} & \cdots & \gamma_{BK}\end{bmatrix} \tag{54}$$

After normalization,

$$R'=\left\{\gamma'_{ij}\right\},\ \gamma'_{ij}=\gamma_{ij}\Big/\sum_{i=1}^{B}\gamma_{ij} \tag{55}$$

The information entropy of the *i-th* parameter is defined as:

$$H_i=-\frac{1}{InB}\sum_{i=1}^{B}\gamma_{ij}In\gamma_{ij}\quad(j=1,2,\ldots,K) \tag{56}$$

Weight is defined as:

$$\varepsilon_i=(1-H_i)\Big/\sum_{i=1}^{K}(1-H_i) \tag{57}$$

3)The comprehensive weight φk is described as follows:

$$\phi_i=(\beta_i/\varepsilon_i)\Big/\left(\sum_{i=1}^{K}\beta_i\Big/\varepsilon_i\right) \tag{58}$$

Because the SBSO algorithm is a heuristic search method, its optimization results have certain randomness. A large number of tests show that the algorithm runs independently for 30 times, the frequency of the minimum value is the largest. If the difference between the values is less than 10^{-7}, these values are regarded as the same number. And the open switches corresponding to the minimum value is the final solution. In this paper, the algorithm runs independently for 50 times each time, and the occurrence times of the minimum value are counted. If the minimum value appears the most times, the minimum value is the optimal solution, otherwise, run independently for 50 times again.

The algorithm flow chart of this paper is shown in Fig.10.

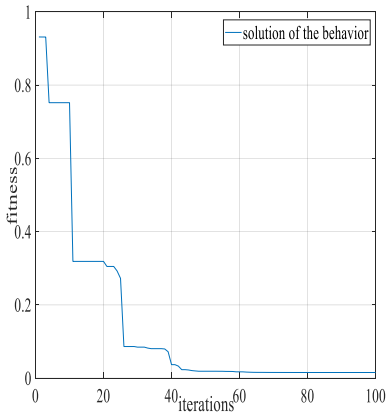

FIGURE 12. The number of iterations.

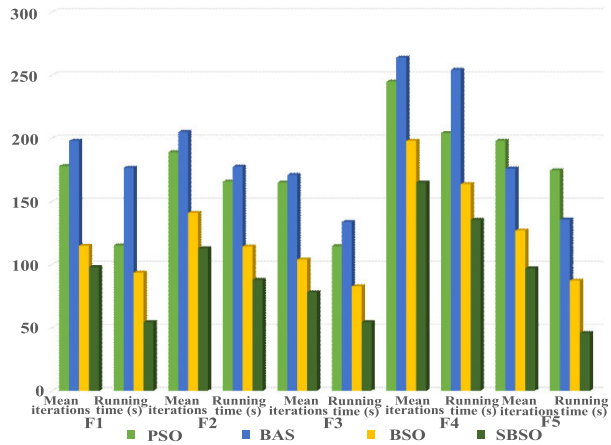

FIGURE 13. The computation cost of five benchmark functions.

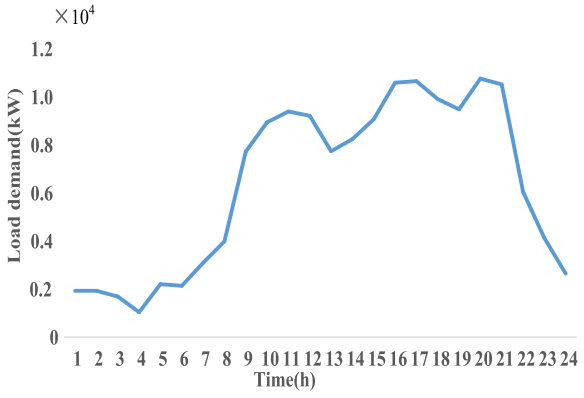

FIGURE 14. Load demand curve based on IEEE-33 node over 24 hours.

C. EXPERIMENTAL DESIGN AND RESUILS ANALYSIS

To preliminarily verify the effectiveness of the SBSO algorithm, it is used to solve the Griewank function. The initial parameters are set as follows: the dimension is 2, the number of beetles is 10, and the number of iterations is 100, $L = 2$, $z_{0,max} = 2.5$, $z_{0,min} = 1.5$, $z_{1,max} = 0.9$, $z_{1,min} = 0.4$ and the social impact factor is 0.01. The SBSO algorithm is used to solve this function, the solving process is shown in the Fig.11, and the number of iterations is shown in the Fig.12.

The SBSO algorithm can effectively find the minimum value of the function, and the minimum value of Griewank can be obtained after approximately 40 iterations with fewer iterations, a fast convergence speed and a high efficiency.

To further verify the superiority of the SBSO algorithm, five representative benchmark functions are simulated and compared with the PSO, BAS, and BSO algorithms. The initial parameters are set as follows: the dimension is 5, the number of beetles is 10, and the number of iteration is 300. Table 6 shows the names of the five benchmark functions, the function expression F, the solution search space range, and minimum value F_{min}, and the dimension D of the variable.

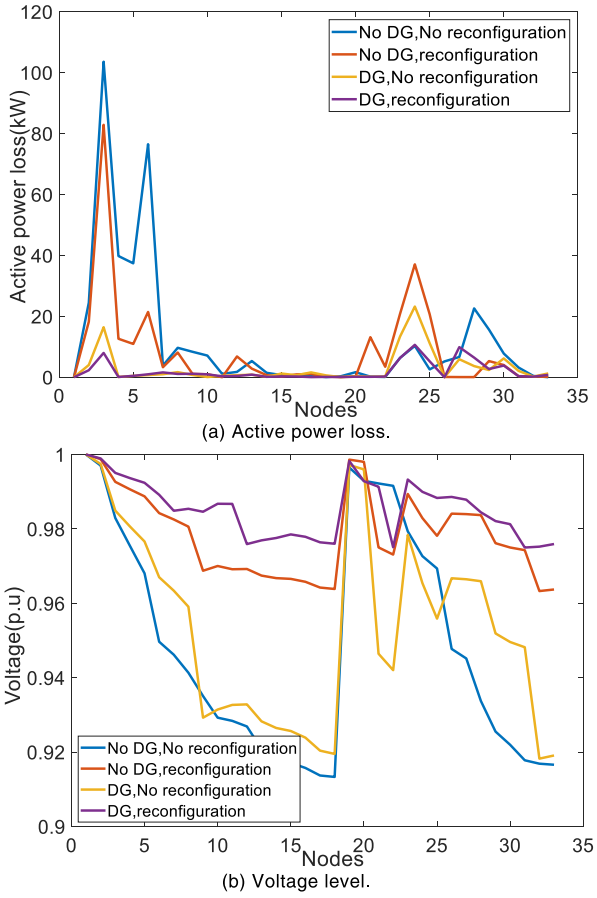

FIGURE 15. The results of different cases.

TABLE 8. Different cases of optimal network reconfiguration.

Case	Definition
1	EV,No DG,No reconfiguration
2	EV,No DG,reconfiguration
3	EV,DG,No reconfiguration
4	EV,DG,reconfiguration

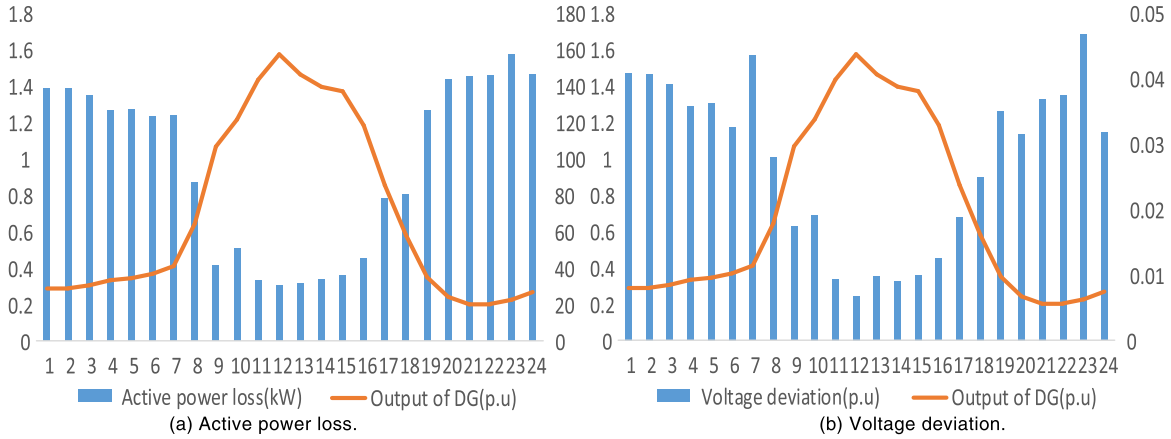

(a) Active power loss. (b) Voltage deviation.

FIGURE 16. Comparison of DG output and optimization objectives.

To ensure the fairness and objectivity of the evaluation, in the test, the four algorithms run independently for 50 times, and the variable dimension is 5. The average values of the experimental results are shown in Table 7.

Table.7 shows that the SBSO algorithm is superior to the PSO, BAS, and BSO algorithms. The BAS algorithm obviously falls into the local optimal value when solving *F1* and *F2*, and can jump out of the local optimal value with a small probability when solving other test functions. Overall, BAS has a limited global optimization ability. The global optimization ability of PSO is better than that of BAS, but it sometimes falls into the local optimal solution. BSO is better than PSO algorithm and BAS algorithm, it can avoid local optimal value in a high probability, but the value obtained by the BSO algorithm is insufficient. By comparison, the SBSO algorithm has the strongest global optimization ability. From Fig.13, PSO and BAS need hundreds of iterations to reach the optimal value, while BSO and SBSO iterations are less than those of PSO and BAS, so the solving efficiency has been significantly improved. The number of iterations of SBSO is less than that of BSO, showing a steady and rapid decline trend in the three test functions. On the other hand, the running time of SBSO algorithm is the least, which means the computational cost of the SBSO algorithm is the least and this algorithm can be computationally efficient to be used in practical applications.

VI. SIMULATION VERIFICATION

The *CPU* model of the computer used in this study was an *Intel (R) core (TM) i5-2400CPU@3.10*. The operating system was Windows 7 ultimate 64 bit, and the running environment was MATLAB 2016a. Based on the abovementioned IEEE-33 node distribution network system. The weight coefficients of the objective function were $\alpha = 2$, $\beta = 1$, $\gamma = 1$, and $\lambda = 2$. The evaluation factors were $a = 0.6$ and $b = 0.4$. The total number of beetles was 50, the maximum number of iterations was 300, $L = 2$, $z_{0,max} = 2.5$, $z_{0,min} = 1.5$, $z_{1,max} = 0.9$, $z_{1,min} = 0.4$, and the social impact factor was 0.01. The scheme before reconfiguration set as one that does not consider the uncertainty of wind power and load, that was to disconnect five tie switches. The original network was to disconnect 33, 34, 35, 36, and 37 switches, without considering network reconfiguration. The total network loss was 3467.45 *kWh*, the voltage deviation was 0.9560 *p.u*, and the load balance was 7.2797 *p.u*. Fig. 14 shows the total demand profile based on IEEE-33 node over 24 hours.

A. DIFFERENT CASES

To validate the presented method and compare it with other methods, the optimal network reconfiguration is solved for the following cases.

Fig.15(*a*) shows that the optimization effects of case 1 and case 2 are similar, those of case 3 and case 4 are close, and the optimization effect of case 4 is obviously better than those of case 1, case 2 and case 3, which means that DG access to the power grid and distribution network reconfiguration can effectively reduce the active power loss.

Fig.15(*b*) shows that the optimization effects of case 3 and case 4 are similar and they are much better than those of case 1 and case 2, indicating that DG can also reduce voltage deviation. The voltage deviation of case 4 is also less than that of case 3, which indicates that the distribution network reconfiguration can reduce the voltage deviation and maintain the voltage level above 0.960 p.u.

Assuming that the load is constant, the DG output changes within 24 hours, the relationship between output of DG and objectives over 24h as shown in Fig. 15.

From Fig.16, with the increase in the output of DG, the active power loss and voltage deviation decrease, which shows that the greater the DG output, the better the grid performance.

B. PARTITION OF TIME INTERVALS

The net load on 33 nodes within 24 hours is analyzed by GRP. When the comprehensive correlation degree is greater than

TABLE 9. Parameters of grey correlation degree.

Time	$\|S_t^0\|$	$\|S_{t+1}^0-S_t^0\|$	$\varepsilon_{t,t+1}$	$\|S_t^1\|$	$\|S_{t+1}^1-S_t^1\|$	$r_{t,t+1}$	$\rho_{t,t+1}$	Time intervals
1	0.088048518			31.05030324				
2	0.088925874	0.000877356	0.999255122	31.05578671	0.005483476	0.999913115	0.999715717	1
3	0.764694674	0.675768799	0.732833223	26.00179604	5.053990676	0.919919748	0.865793791	
4	0.536718494	0.22797618	0.909869084	25.62074097	0.381055072	0.992810769	0.967928263	
5	2.535461863	1.99874337	0.670767834	20.7482236	4.872517363	0.906730874	0.835941962	
6	1.941400959	0.594060904	0.902146538	22.41082934	1.662605735	0.963715723	0.945244968	2
7	1.750509393	0.190891566	0.960905323	24.85319551	2.442366169	0.951833169	0.954554815	
8	0.626482156	1.124027237	0.750272707	28.75977179	3.906576283	0.93324322	0.878352066	
9	4.299116456	3.6726343	0.617363495	38.61154048	9.851768693	0.874055476	0.797047882	
10	5.073656917	0.774540461	0.930517749	38.81747036	0.205929873	0.997381191	0.977322158	
11	4.180129197	0.89352772	0.919843674	36.64724882	2.170221536	0.972401308	0.956634018	
12	2.971108593	1.209020604	0.870834698	34.68465999	1.962588828	0.973583658	0.94275897	
13	1.675922721	1.295185872	0.813433398	33.20310116	1.481558828	0.978945955	0.929292188	3
14	2.821206287	1.145283566	0.827580182	35.05033272	1.847231558	0.97401949	0.930087698	
15	3.93573169	1.114525403	0.87436961	36.55497183	1.50463911	0.979697203	0.948098925	
16	4.430162624	0.494430934	0.949856529	36.48670625	0.068265582	0.999078861	0.984312161	
17	3.259220776	1.170941849	0.881247137	34.78844839	1.69825786	0.977042321	0.948303766	
18	0.681755847	2.577464928	0.657180958	31.3853972	3.403051184	0.951782363	0.863401942	
19	1.859512495	1.177756648	0.750423732	28.20430556	3.181091643	0.950116794	0.890208876	
20	1.968578186	0.10906569	0.977909209	28.33672727	0.132421707	0.99770394	0.991765521	4
21	2.87896261	0.910384424	0.865286402	27.37069282	0.966034453	0.983249929	0.947860871	
22	3.077054452	0.198091842	0.972310759	25.1947337	2.175959112	0.960963311	0.964367546	
23	2.854383828	0.222670624	0.968875142	23.70384803	1.490885675	0.970988497	0.970354491	
24	0.702040895	2.152342933	0.67917462	27.57482961	3.870981577	0.931059571	0.855494086	5

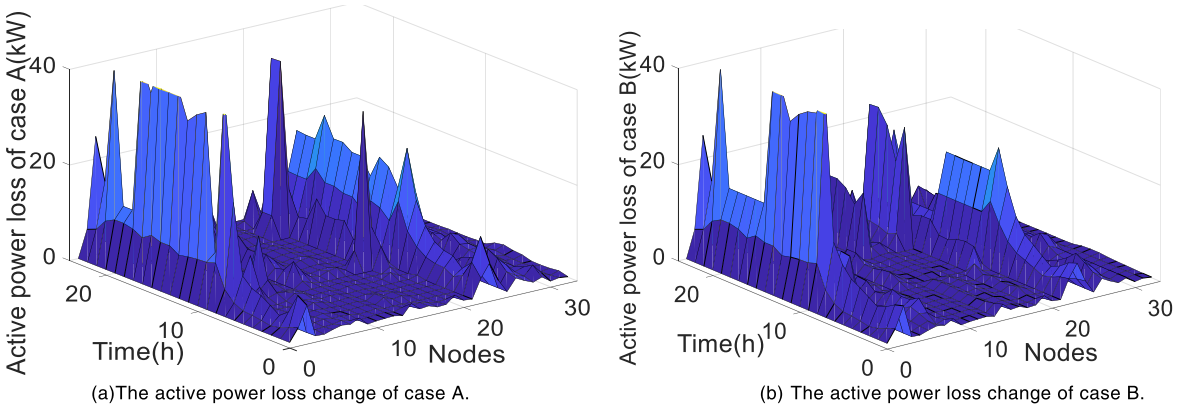

FIGURE 17. The active power loss change of each node in 24h.

0.865, the time interval can be merged. The combined results are shown in the Table 9.

Case *A* is reconfiguration twenty-four times over 24 hours, case *B* is reconfiguration five times over 24 hours.

Case *A* compared with case *B*. The results in each node are shown in the Figs.17 and 18.

From Figs.17 and 18, active power loss, load balancing and maximum node voltage deviation on 33 nodes over 24 hours of case *A* are similar to case *B*. The results of case *A* and case *B* in 24h are shown in Table 10 and Fig.19.

From Fig.19, active power loss, load balancing and maximum node voltage deviation over 24 hours of case *A* are

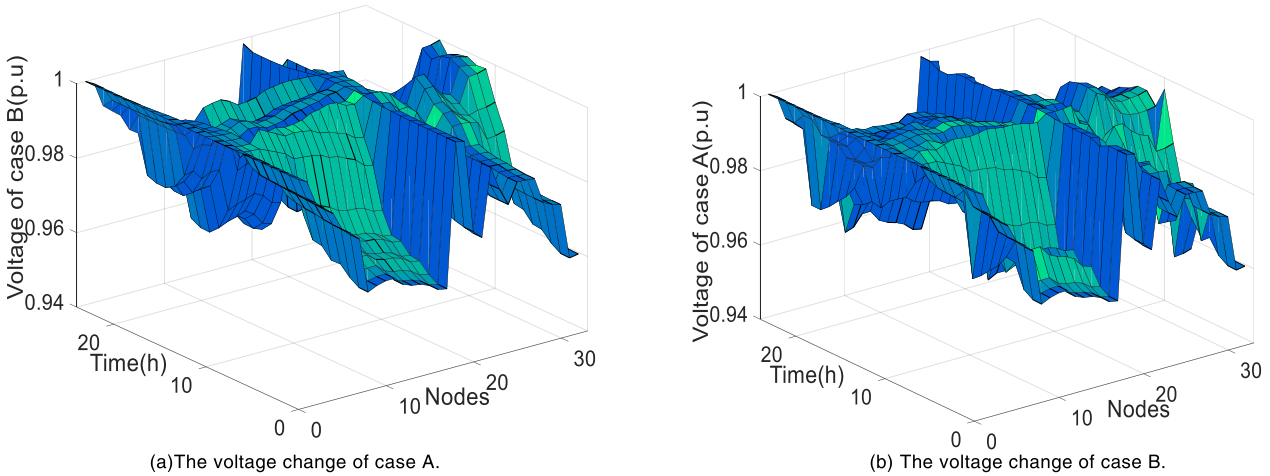

(a)The voltage change of case A. (b) The voltage change of case B.

FIGURE 18. The voltage change of each node in 24h.

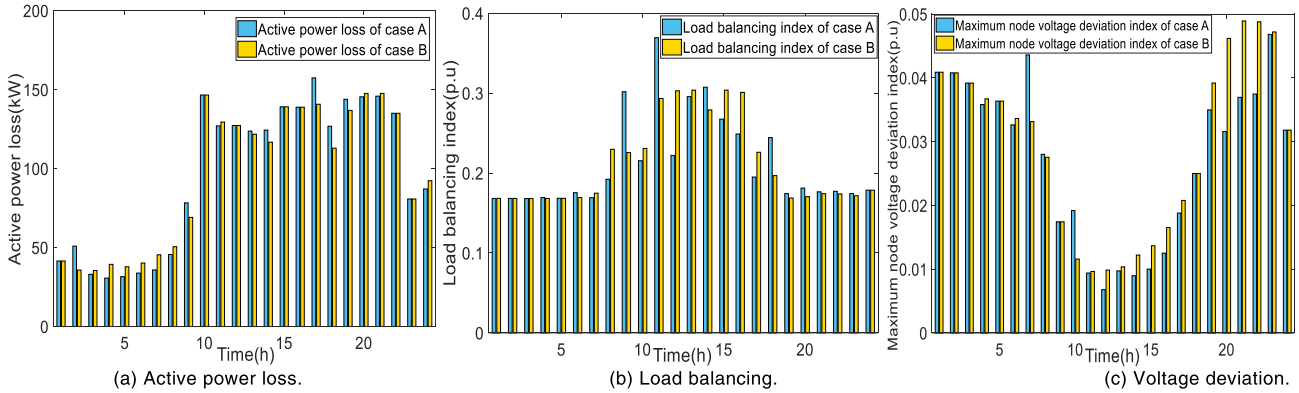

(a) Active power loss. (b) Load balancing. (c) Voltage deviation.

FIGURE 19. The results of case A and case B in 24h.

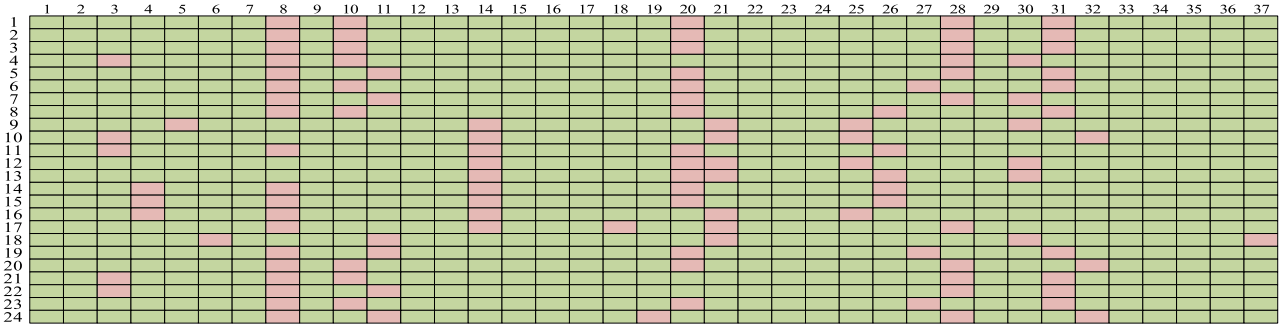

FIGURE 20. Switch distribution diagram of Case A.

similar to case B, it is only that the load balance and voltage deviation of case B are slightly larger than that of case A, the load balance degree of case B is 0.0072884 larger than that of case A, and the voltage deviation of case B is 0.0427327 larger than that of case A, which only affects the power grid performance and voltage quality in the permissible range. In contrast, the active power loss of case B is less than that of case A.

The network loss of distribution network will cause extra cost which is obtained by active power loss f^1 and electricity price $C_1(\$220.92/MW*h)$. And cost of the switching operation is obtained by the number of switching operation f_s and the cost of per switching operation $C_2(\$147.28/per)$. Based on this, the total cost of case A is $\$522812.6811$, the total cost of case B is $\$511835.805$, so case B cut down the unnecessary expense of $\$10976.8761$, which is more economical.

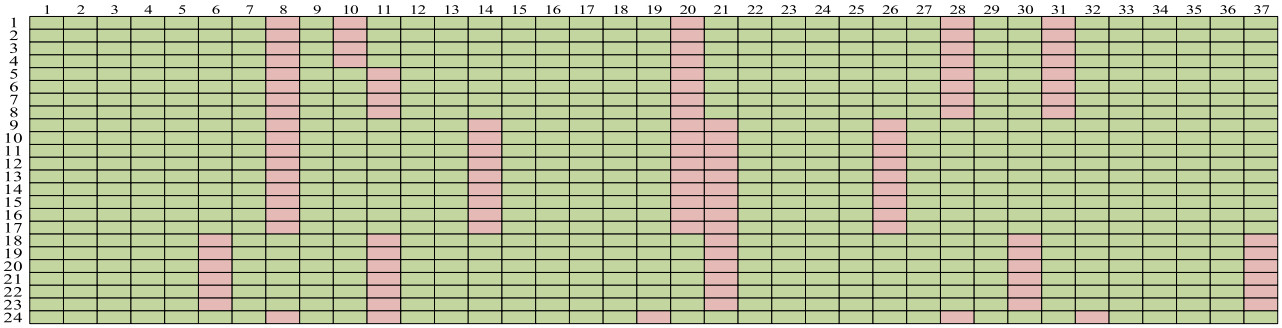

FIGURE 21. Switch distribution diagram of Case B.

TABLE 10. The results of case A and case B over 24h.

Time(h)	Active power loss(kW)		Load balancing index(p.u)		Maximum node voltage deviation index(p.u)		Open switches	
	Case A	case B	Case A	case B	Case A	case B	Case A	case B
1	41.49392556	41.49392556	0.168268447	0.168268447	0.0408842	0.0408842	[20,10,8,31,28]	[20,10,8,31,28]
2	50.90895072	35.74611844	0.168248975	0.168248975	0.0407838	0.0407838	[20,10,8,31,28]	
3	33.04068233	35.43658973	0.168060421	0.168060421	0.0391839	0.0391839	[20,10,8,31,28]	
4	30.65857796	39.36903265	0.169362416	0.168216993	0.0358115	0.0367105	[3,10,8,30,28]	
5	31.57864318	37.84396063	0.168416021	0.168416021	0.0363533	0.0363533	[20,11,8,31,28]	[20,11,8,31,28]
6	33.81996872	40.17071207	0.175410056	0.169394718	0.0326215	0.0336200	[20,10,8,31,27]	
7	35.82305268	45.42723298	0.169113528	0.174816911	0.0435983	0.0331539	[20,11,8,30,28]	
8	45.59728656	50.52903054	0.192207511	0.229739881	0.0280148	0.0275486	[20,10,8,31,26]	
9	78.29066255	69.11173409	0.301759762	0.225636093	0.0174310	0.0174310	[5,14,21,30,25]	[20,14,21,8,26]
10	146.5886240	146.5886240	0.21541998	0.230809228	0.0191898	0.0115921	[3,14,21,32,25]	
11	127.0461154	129.4940455	0.369368709	0.293314075	0.0093954	0.0096456	[20,14,3,8,26]	
12	127.2946718	127.2946780	0.222057671	0.302941598	0.0067950	0.0098584	[20,14,21,30,26]	
13	123.7306375	121.7695174	0.295602656	0.303763517	0.0097345	0.0103706	[20,14,21,30,25]	
14	124.3672077	116.7114934	0.307379973	0.279009036	0.0089755	0.0122118	[20,14,4,8,26]	
15	139.1132918	139.1132918	0.267433669	0.303773947	0.0100086	0.0136730	[20,14,4,8,26]	
16	138.8659585	138.8659585	0.248849945	0.30095239	0.0125136	0.0165239	[4,14,21,8,25]	
17	157.4279337	140.7444617	0.194998519	0.226016381	0.0187977	0.0207862	[18,14,21,8,28]	
18	126.8181379	112.9464862	0.244335757	0.196780126	0.0250061	0.0250061	[6,11,21,30,37]	[6,11,21,30,37]
19	143.8867475	136.8532903	0.17423042	0.168692178	0.0349810	0.0391882	[20,11,8,31,27]	
20	145.4356537	147.6085808	0.181167963	0.170449462	0.0315798	0.0461840	[20,10,8,32,28]	
21	145.8631467	147.6085808	0.176525891	0.174157299	0.0369440	0.0489178	[3,10,8,31,28]	
22	135.0314483	135.0314483	0.177203426	0.173935707	0.0374582	0.0487848	[3,11,8,31,28]	
23	80.75532203	80.75532203	0.174299445	0.171616209	0.0468136	0.0471964	[20,10,8,31,27]	
24	87.09237494	92.32771702	0.178589997	0.178589997	0.0318036	0.0318032	[19,11,8,32,28]	[19,11,8,32,28]
Total	2330.529028	2308.841832	5.108311159	5.115599609	0.654678705	0.697411402	Numbers of switching operations	
							54	12

Green and red represent connection and disconnection in the distribution network respectively.

The switch distribution diagram of case *A* and case *B* are shown in Figs.20 and 21.

It clearly shows that case *B* causes a substantial reduction in the number of switching operations.

If the wind speed and solar radiation are predicted, the DG output will be obtained. The data series is reconstructed

TABLE 11. Parameters of GTDM.

Time	Mean value of effect value			The centre of the grey target		
	$t^{(1)}$	$t^{(2)}$	$t^{(3)}$	$R_1{}^0$	$R_2{}^0$	$R_3{}^0$
1	43.4531037	0.169098909	0.0425925	0.0207904	0.0204233	0.0209571
2	42.1461942	0.168248987	0.040827621	0.0204082	0.0204082	0.0204082
3	34.2372252	0.168031843	0.039314647	0.0638298	1.0000000	0.0638298
4	31.6751111	0.195905853	0.04754568	0.2102814	0.2343844	0.3120481
5	33.0242984	0.169452032	0.038080215	0.0204082	0.0204082	0.0204082
6	35.4395271	0.169459019	0.033010858	0.4797547	0.2620302	0.5491110
7	36.6087851	0.17163021	0.045732984	0.0754295	0.0954661	0.2047520
8	48.1215881	0.196779385	0.033506218	0.1294034	0.1489237	0.2102378
9	87.0712662	0.307314263	0.018740525	0.2761843	1.0000000	0.2713609
10	119.5541346	0.253746787	0.018039544	0.1097564	1.0000000	0.1035250
11	177.5462062	0.383054267	0.009434717	0.2898418	0.2393101	0.1296888
12	137.221537	0.236359671	0.007596255	0.1533839	0.1421998	0.1927855
13	122.1014182	0.313526174	0.00988439	0.2368106	0.1880017	0.0758121
14	139.8615388	0.32951546	0.00900764	0.2352199	0.2263206	0.2359269
15	149.3892061	0.274521464	0.010054426	0.0835549	0.0856780	0.0277062
16	139.0507396	0.267998993	0.01256354	0.3160852	0.2435202	0.3180155
17	178.7575222	0.217929749	0.021510115	0.0762828	0.2312796	0.0649317
18	167.7107542	0.254823117	0.027812447	0.4257314	0.1997435	0.2260438
19	165.444285	0.184590208	0.041913924	0.1438204	0.1163709	0.2122574
20	146.0377698	0.192662028	0.042058172	0.2393098	0.1697528	0.2384018
21	167.0339696	0.176521335	0.037249214	0.2785339	1.0000000	0.2209700
22	135.5685421	0.178676391	0.040978134	0.0703830	0.0396994	0.0664856
23	102.9265243	0.19313678	0.062277961	0.3683119	0.4337612	0.4484025
24	111.1813665	0.209553117	0.06545024	0.4405579	0.2933087	0.5008563

by the above-mentioned GRP. It can be known that the switching operation can be carried out as soon as possible in a reconstruction period to avoid multiple complex operations each hour. The simulation results show that the proposed method can greatly reduce the switching operations and reduce the total cost of distribution network reconfiguration.

C. GREY TARGET DECISION-MAKING

GTDM uses objective data to determine the ideal scheme as the target center. By calculating the target distance between the candidate scheme and the ideal scheme, the smaller the target distance is, the better the effect is. The grey decision theory is integrated into the SBSO algorithm to solve the multiobjective optimization problem, which avoids the subjectivity and objectivity of directly weighting the target value. The average effect and the center of GTDM in the algorithm are shown in Table 11.

From Fig.22, The average effect value has the same trend with the real parameters of distribution network reconfiguration in 24h, which can reflect the reconfiguration effect to a certain extent.

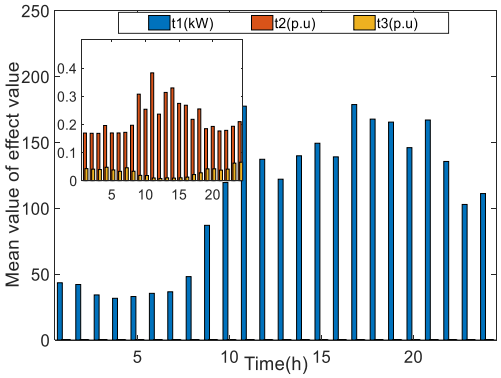

FIGURE 22. The mean value of effect value.

The algorithm based on the GTDM method and the algorithm based on the entropy weight method are used to solve the distribution network reconfiguration problem.

TABLE 12. The results of two methods based on IEEE 33-node.

Time	Active power loss(kW)		Load balancing index(p.u)		Maximum node voltage deviation index(p.u)	
	Grey target	Weight factors	Grey target	Weight factors	Grey target	Weight factors
1	41.4939256	99.9706051	0.168268447	0.309678621	0.040884231	0.045517524
2	50.9089507	113.2275589	0.168248975	0.369588659	0.040783786	0.048991852
3	33.0406823	93.73135118	0.168060421	0.37318584	0.03918386	0.046088265
4	30.658578	88.01082671	0.169362416	0.302050221	0.035811526	0.041636538
5	31.5786432	92.6621942	0.168416021	0.354549783	0.036353346	0.047553398
6	33.8199687	91.03033645	0.175410056	0.229520795	0.032621533	0.034664652
7	35.8230527	96.32451574	0.169113528	0.243967822	0.043598291	0.025527179
8	45.5972866	115.0493323	0.192207511	0.360796369	0.028014826	0.017873258
9	78.2906626	115.9140026	0.301759762	0.310085209	0.017430959	0.036838243
10	146.588624	229.3159858	0.21541998	0.293379911	0.019189754	0.024358544
11	127.0461154	187.6508605	0.369368709	0.318230318	0.0093954	0.018485885
12	127.294678	129.5693169	0.222057671	0.213469042	0.006795043	0.015478242
13	123.7306375	131.3684739	0.295602656	0.247897603	0.009734538	0.021189357
14	124.3672077	120.7813083	0.307379973	0.282791373	0.008975504	0.017945808
15	139.1132918	164.0546164	0.267433669	0.239328094	0.0100086	0.022742293
16	138.8659585	172.9015693	0.248849945	0.273820818	0.012513599	0.024589996
17	157.4279337	159.7367884	0.194998519	0.267805587	0.018797674	0.026518148
18	126.8181379	163.8306907	0.244335757	0.368622129	0.025006116	0.048958818
19	143.8867475	164.5663677	0.17423042	0.315390586	0.034981017	0.044273792
20	145.4356537	164.3728074	0.181167963	0.168692337	0.031579842	0.041616912
21	145.8631467	187.0341367	0.176525891	0.321984948	0.036943982	0.038377696
22	135.0314483	173.0244149	0.177203426	0.257081227	0.037458286	0.027255059
23	80.755322	108.3586768	0.174299445	0.318735207	0.046813697	0.047782616
24	87.0923749	108.5831962	0.178589997	0.339856242	0.031803296	0.02784087
Total	2330.529028	2780.825341	5.108311159	7.08050874	0.654678705	0.792104945

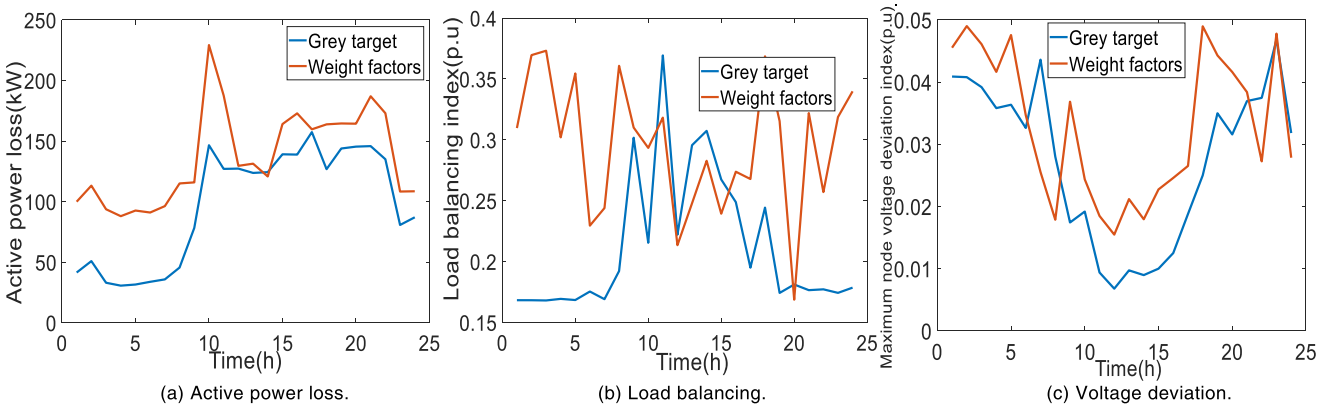

(a) Active power loss. (b) Load balancing. (c) Voltage deviation.

FIGURE 23. The results of two methods based on IEEE-33nodes.

The weights of active power loss, voltage deviation and load balance are 0.5, 0.3, and 0.2, respectively. The results are as follows.

From Fig.23, the SBSO algorithm based on GTDM has obvious advantages in solving multiobjective distribution network reconfiguration, active power loss,

TABLE 13. Detail comparison based on IEEE-33 node with PSO, BAS, BSO algorithm.

Time(h)	Active power loss(kW)				Maximum node voltage deviation index(p.u)				Load balancing index(p.u)			
	PSO in [34]	BAS in [32]	BSO	SBSO	PSO in [34]	BAS in [32]	BSO	SBSO	PSO in [34]	BAS in [32]	BSO	SBSO
1	49.79271	88.73112	86.91537	41.49393	0.04497	0.02916	0.03300	0.04088	0.20192	0.29294	0.37404	0.16827
2	61.09074	83.05403	84.57462	50.90895	0.04486	0.02943	0.03983	0.04078	0.20190	0.28226	0.23143	0.16825
3	39.64882	180.35809	80.48966	33.04068	0.04310	0.02880	0.03493	0.03918	0.20167	0.28922	0.41203	0.16806
4	36.79029	151.51231	87.75649	30.65858	0.03939	0.03245	0.03531	0.03581	0.20323	0.24432	0.19647	0.16936
5	37.89437	86.33643	87.64421	31.57864	0.03999	0.03052	0.04044	0.03635	0.20210	0.26513	0.13779	0.16842
6	40.58396	86.20677	73.79525	33.81997	0.03588	0.02913	0.03773	0.03262	0.21049	0.28414	0.15192	0.17541
7	42.98766	89.50075	111.59184	35.82305	0.04796	0.03213	0.04089	0.04360	0.20294	0.25858	0.48014	0.16911
8	54.71674	96.92740	65.10027	45.59729	0.03082	0.02966	0.03383	0.02801	0.23065	0.23280	0.35871	0.19221
9	93.94880	133.99846	83.28927	78.29066	0.01917	0.02801	0.02004	0.01743	0.36211	0.19574	0.21973	0.30176
10	175.90635	119.11951	126.84006	146.58862	0.02111	0.03209	0.02443	0.01919	0.25850	0.15805	0.14624	0.21542
11	152.45534	118.11576	128.64768	127.04612	0.01033	0.02520	0.02208	0.00940	0.44324	0.28850	0.17504	0.36937
12	152.75361	125.06173	145.41897	127.29468	0.00747	0.02106	0.02399	0.00680	0.26647	0.23602	0.31654	0.22206
13	148.47677	129.70084	126.90002	123.73064	0.01071	0.03831	0.02719	0.00973	0.35472	0.14356	0.13531	0.29560
14	149.24065	120.24285	139.05120	124.36721	0.00987	0.03365	0.02336	0.00898	0.36886	0.15650	0.13034	0.30738
15	166.93595	131.72188	127.51461	139.11329	0.01101	0.03404	0.03257	0.01001	0.32092	0.16932	0.23572	0.26743
16	166.63915	131.67162	162.30085	138.86596	0.01376	0.03554	0.02116	0.01251	0.29862	0.19548	0.18387	0.24885
17	188.91352	133.05552	92.71807	157.42793	0.02068	0.03936	0.02539	0.01880	0.23400	0.25519	0.19397	0.19500
18	152.18177	139.18551	44.96899	126.81814	0.02751	0.03037	0.02470	0.02501	0.29320	0.28456	0.13847	0.24434
19	172.66410	125.34939	105.60263	143.88675	0.03848	0.02804	0.01301	0.03498	0.20908	0.30466	0.23856	0.17423
20	174.52278	126.58864	125.80764	145.43565	0.03474	0.03060	0.02947	0.03158	0.21740	0.26278	0.13573	0.18117
21	175.03578	125.34939	127.41843	145.86315	0.04064	0.03026	0.03401	0.03694	0.21183	0.27747	0.23820	0.17653
22	162.03774	131.02279	145.66566	135.03145	0.04120	0.03060	0.03344	0.03746	0.21264	0.26278	0.19247	0.17720
23	96.90639	119.36404	94.46130	80.75532	0.05150	0.02843	0.02533	0.04681	0.20916	0.29560	0.26007	0.17430
24	104.51085	97.66234	117.36989	87.09237	0.03498	0.03192	0.03249	0.03180	0.21431	0.24834	0.36416	0.17859
Total	2796.63483	2869.83718	2571.84178	2330.52903	0.72015	0.73876	0.70859	0.65468	6.12997	5.88394	5.64694	5.10831

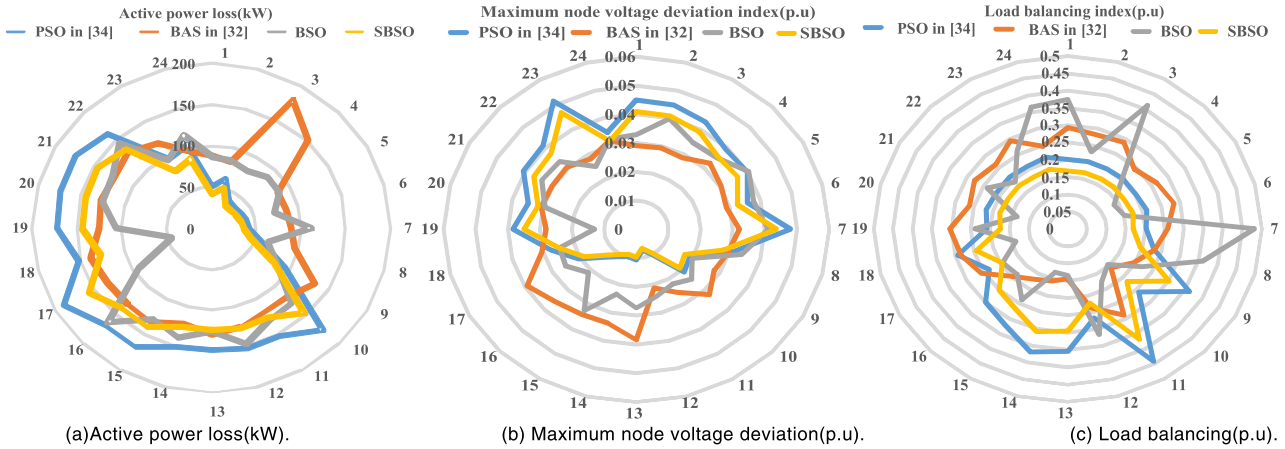

(a)Active power loss(kW). (b) Maximum node voltage deviation(p.u). (c) Load balancing(p.u).

FIGURE 24. Detail comparison based on IEEE-33 node with PSO, BAS, BSO algorithm.

Load balancing index and maximum node voltage deviation index are less than the algorithm based on the entropy weight method. SBSO algorithm based on GTDM is a more effective multiobjective algorithm, which can find the optimal solution of multiple objectives simultaneously.

TABLE 14. The results based on IEEE-33 node compared with PSO, BAS, BSO algorithm.

Algorithm	Active power loss(kWh)	Maximum node voltage deviation index(p.u)	Load balancing index(p.u)	Iterations	Running time(s)
PSO in [34]	2796.63483	0.72015	6.12997	103	226.49462
BAS in [32]	2869.83718	0.73876	5.88394	148	279.56482
BSO	2571.84178	0.70859	5.64694	76	197.86465
SBSO	2330.52903	0.65468	5.10831	67	176.56489

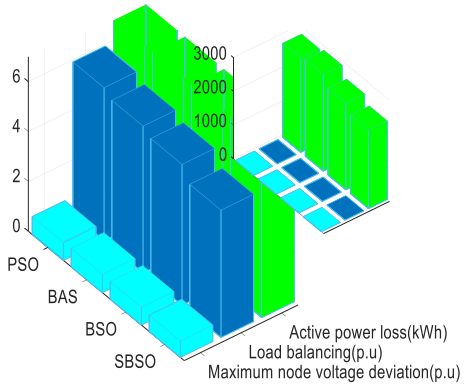

FIGURE 25. The results based on IEEE-33 node.

D. DIFFERENT ALGORITHM

For case 4 of the IEEE-33 system, the reconfiguration strategy of the algorithm in this paper is used to reconstruct the distribution network, and the active power loss, voltage deviation and load balance are recorded. The detail results are compared with those of the PSO in [34], BAS in [32], and BSO algorithm in Table 13 and Fig. 24.

Table 13 and Fig.24 show that SBSO and BSO have smaller values than BAS and PSO. Although the results obtained by SBSO algorithm is not the smallest in 24 hours, which is related to the power grid state at that time, it can be seen from the Fig.24 that the surface enclosed by SBSO algorithm is closer to the origin, and its value is optimal.

TABLE 15. The specific parameters and the locations of DG access to IEEE 69-node.

Type	Location	Capacity/kW	Power factor
photovoltaic panels	26	400	0.95
Wind turbine	39	500	0.95
photovoltaic panels	54	350	0.95
Wind turbine	68	450	0.95

Table 14 and Fig.25 show that SBSO and BSO have smaller values than those of BAS and PSO, and Fig.26 shows that the SBSO more easily finds smaller global optimal solutions in a shorter time. And the number of iterations is substantially fewer for SBSO than for the other three algorithms, and the fitness value is smaller, which means the computation cost of the proposed approach is the least.

The BSO algorithm combines the advantages of the PSO and BAS, improves the efficiency of the PSO algorithm, and helps the BAS jump out of the local optimal solution to a great extent. The above results also verify this conclusion. BSO has a better global search ability and higher solution efficiency than those of PSO and BAS. Based on BSO, this algorithm improves its operator, adds social learning progress, and sorts and updates each optimization result to form an improved SBSO algorithm. From the above results, it is apparent that the SBSO algorithm has a stronger global search ability than the BSO algorithm, and it can find the global optimal value

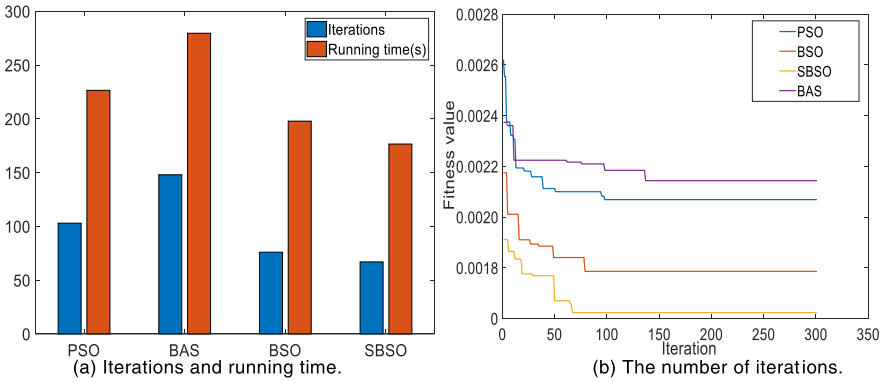

FIGURE 26. The computation cost based on IEEE-33 node.

TABLE 16. The results of two methods based on IEEE 69-node.

Time(h)	Open switches		Active power loss(kW)		Maximum node voltage deviation index(p.u)		Load balancing index(p.u)	
	Grey target	Weight factors	Grey target	Weight factors	Grey target	Weight factors	Grey target	Weight factors
1	[10,70,14,41,35]	[10,18,67,41,36]	56.83054927	108.164525	0.100493166	0.116397915	0.358807956	0.448107075
2	[10,70,14,41,36]	[10,14,66,42,35]	68.15268399	107.0554352	0.100453143	0.115807442	0.362443321	0.449308907
3	[10,70,14,41,36]	[10,14,67,43,35]	74.23268331	108.7120733	0.099499309	0.116915736	0.365389724	0.450290214
4	[10,70,14,41,35]	[10,17,66,42,35]	73.75529904	103.1923586	0.097991061	0.111241541	0.370312132	0.452204844
5	[10,70,14,41,35]	[10,17,12,41,36]	58.52938397	157.4870711	0.097395755	0.107814895	0.372393075	0.389145847
6	[10,70,14,41,35]	[10,14,67,43,35]	82.56160455	104.8424226	0.095730106	0.107520524	0.378569532	0.45669876
7	[10,70,13,41,35]	[10,14,67,42,36]	92.68418512	92.23452073	0.090945149	0.100175664	0.373815025	0.456795843
8	[10,70,12,41,35]	[10,13,12,42,35]	97.11413309	100.3211504	0.065755299	0.066439528	0.376043422	0.37637153
9	[10,13,11,41,36]	[8,15,68,48,41]	196.8928598	192.5448414	0.036795858	0.06661897	0.586103931	0.744468472
10	[9,13,11,41,36]	[8,13,11,41,36]	194.2951355	158.7916564	0.031244071	0.034710206	0.548921438	0.54395009
11	[8,13,11,41,36]	[10,14,68,41,35]	190.0044767	175.0651108	0.023488735	0.0194489	0.539646239	0.543929143
12	[69,16,13,41,36]	[9,17,68,42,35]	188.0753542	185.1706848	0.034278709	0.025960084	0.75367913	0.560215955
13	[8,13,11,41,36]	[10,14,68,41,36]	187.9808273	202.9061251	0.022218961	0.018395638	0.472522965	0.472654378
14	[9,16,13,41,36]	[9,14,68,42,36]	186.4933676	200.6396558	0.01999576	0.026336668	0.419305236	0.430380685
15	[9,17,13,41,36]	[8,13,11,41,36]	184.2632393	216.0534564	0.020946242	0.030927747	0.376581654	0.3841159
16	[10,19,13,41,35]	[10,17,13,41,36]	183.4032647	224.3285017	0.03046504	0.033800891	0.355961498	0.369385289
17	[10,70,12,41,36]	[8,18,12,49,44]	181.0927364	205.8040464	0.062607702	0.1012344	0.432867324	0.543387842
18	[10,70,14,41,35]	[9,14,67,41,36]	208.4229363	239.708063	0.083050043	0.080469568	0.441109385	0.609932042
19	[10,70,14,41,35]	[10,14,67,41,35]	176.8038915	177.3836503	0.096800705	0.108786652	0.374539358	0.453056641
20	[10,70,14,41,36]	[10,17,67,41,36]	173.7577405	179.166701	0.103293767	0.12278043	0.354562816	0.449032967
21	[10,70,14,41,36]	[10,14,66,42,35]	205.8186264	226.4770263	0.105768014	0.129029467	0.348695733	0.452242847
22	[10,70,14,41,36]	[10,17,12,41,35]	163.460208	168.5911016	0.105648407	0.11609382	0.348959718	0.359344511
23	[10,70,14,41,36]	[10,17,12,41,35]	130.8296889	134.9298656	0.104213745	0.114648033	0.352279205	0.363562803
24	[10,70,14,41,36]	[7,14,66,42,36]	110.8833675	113.5171671	0.101705811	0.168848543	0.358807956	0.422818069
Total			3466.338243	3883.087211	1.730784492	2.040403255	10.02231777	11.18140066

with higher efficiency and the highest accuracy in fewer iterations.

E. SCALABILITY

The SBSO algorithm is used to reconstruct the standard IEEE-69 node distribution network in 24 hours. The parameters of the DG type, capacity and access node are shown in Table 15 [36]. In Fig. 27 shows the total demand profile based on IEEE-69 node over 24 hours.

The results compared with weight factors are shown in the Table 16 and Fig.28.

From Fig.28, the SBSO algorithm based on GTDM has obvious advantages in solving multiobjective distribution network reconfiguration, active power loss, load balancing index and maximum node voltage deviation index are less than those of algorithm based on the entropy weight method simultaneously. The results obtained by SBSO algorithm based on GTDM is almost the smallest in 24 hours. From Fig.28, the surface enclosed by SBSO algorithm based on GTDM is closer to the origin, and its value is optimal.

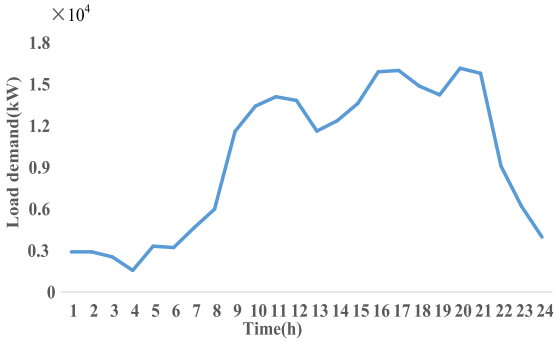

FIGURE 27. Load demand curve based on IEEE-69 node over 24 hours.

TABLE 17. The open switches of four algorithms.

Open switches									
Time(h)	PSO in [34]	BAS in [32]	BSO	SBSO	Time(h)	PSO in [34]	BAS in [32]	BSO	SBSO
1	[59,13,68,48,47]	[65,13,67,44,36]	[3,15,68,42,8]	[10,70,14,41,35]	13	[4,19,71,43,36]	[9,14,67,42,36]	[58,15,14,10,47]	[8,13,11,41,36]
2	[64,17,12,46,36]	[61,70,13,49,42]	[58,18,13,51,47]	[10,70,14,41,36]	14	[7,17,71,42,36]	[64,15,68,24,47]	[59,13,11,22,4]	[9,16,13,41,36]
3	[10,16,13,43,36]	[5,18,71,41,38]	[64,15,71,50,42]	[10,70,14,41,36]	15	[64,13,71,42,38]	[6,14,66,24,46]	[9,14,58,15,6]	[9,17,13,41,36]
4	[9,70,11,49,8]	[6,16,68,42,37]	[7,19,13,11,43]	[10,70,14,41,35]	16	[8,16,14,53,45]	[62,15,67,43,35]	[6,14,11,25,46]	[10,19,13,41,35]
5	[8,18,67,49,42]	[69,70,59,42,73]	[59,18,11,41,38]	[10,70,14,41,35]	17	[60,17,66,49,46]	[64,19,13,25,35]	[8,19,68,23,46]	[10,70,12,41,36]
6	[62,14,68,41,73]	[60,15,13,49,47]	[58,16,11,52,4]	[10,70,14,41,35]	18	[4,13,71,42,37]	[64,17,14,46,36]	[59,16,71,12,36]	[10,70,14,41,35]
7	[10,17,11,13,8]	[6,14,12,47,36]	[59,16,66,49,8]	[10,70,13,41,35]	19	[61,16,12,47,35]	[5,13,67,43,73]	[3,70,68,41,43]	[10,70,14,41,35]
8	[63,18,14,48,45]	[8,17,12,43,36]	[9,15,68,12,37]	[10,70,12,41,35]	20	[3,17,68,48,46]	[8,13,11,23,35]	[65,19,11,22,41]	[10,70,14,41,36]
9	[6,13,11,49,73]	[9,16,67,46,37]	[8,14,68,51,47]	[10,13,11,41,36]	21	[65,13,11,72,41]	[64,15,11,25,47]	[65,14,68,11,8]	[10,70,14,41,36]
10	[7,18,66,43,36]	[10,17,12,26,46]	[59,13,68,53,35]	[9,13,11,41,36]	22	[59,15,68,45,36]	[6,70,67,46,37]	[62,13,68,43,5]	[10,70,14,41,36]
11	[61,16,12,47,36]	[9,17,14,25,41]	[9,18,61,14,8]	[8,13,11,41,36]	23	[59,16,14,48,45]	[10,19,11,24,42]	[58,19,66,24,42]	[10,70,14,41,36]
12	[5,15,11,20,44]	[10,14,11,23,35]	[65,13,67,11,6]	[69,16,13,41,36]	24	[63,16,66,41,36]	[9,13,66,25,46]	[4,17,12,22,35]	[10,70,14,41,36]

TABLE 18. Detail comparison based on IEEE-69 node with PSO, BAS, BSO algorithm.

Time(h)	Active power loss(kW)				Maximum node voltage deviation index(p.u)				Load balancing index(p.u)			
	PSO in [34]	BAS in [32]	BSO	SBSO	PSO in [34]	BAS in [32]	BSO	SBSO	PSO in [34]	BAS in [32]	BSO	SBSO
1	61.29166	89.34093	72.39137	56.83055	0.04238	0.40061	0.08665	0.10050	0.62075	1.39238	0.74477	0.35881
2	67.16281	86.18085	83.59203	68.15268	0.05723	0.02963	0.06983	0.10046	0.74059	0.39691	0.61072	0.36244
3	67.42918	84.33172	86.38371	74.23268	0.06941	0.03085	0.05805	0.09950	0.42116	0.38965	0.40963	0.36539
4	60.56998	81.32355	86.88644	73.75530	0.07105	0.07179	0.07522	0.09799	0.46067	0.35937	0.63790	0.37031
5	67.06352	96.87960	89.26464	58.52938	0.06172	0.02479	0.07411	0.09740	0.64067	1.10453	0.48410	0.37239
6	85.75510	93.49895	69.09371	82.56160	0.05344	0.20786	0.06423	0.09573	0.83132	0.34396	0.73948	0.37857
7	115.90923	93.98877	94.28122	92.68419	0.06499	0.07797	0.32477	0.09095	0.29898	0.54780	0.24754	0.37382
8	121.70285	104.36588	109.26815	97.11413	0.03204	0.10643	0.03924	0.06576	0.31420	0.46677	0.54261	0.37604
9	210.31025	187.09172	194.81537	196.89286	0.01106	0.01763	0.06700	0.03680	0.67147	0.37964	0.38618	0.58610
10	215.35443	181.12512	179.57991	194.29514	0.05744	0.06577	0.02171	0.03125	0.28272	0.49084	0.60572	0.54892
11	199.00954	204.65796	192.84632	190.00448	0.07246	0.08030	0.02877	0.02349	0.40347	0.38647	0.77550	0.53965
12	211.14312	225.77932	222.79816	188.07535	0.07560	0.02508	0.10893	0.03428	0.44587	0.52922	0.37552	0.75368
13	210.70590	235.15928	226.18617	187.98083	0.02205	0.10877	0.03086	0.02222	0.58968	0.34621	0.43389	0.47252
14	211.81128	191.02597	201.63384	186.49337	0.05858	0.06407	0.02397	0.02000	0.32688	0.37980	0.37226	0.41931
15	200.02763	213.44820	205.13808	184.26324	0.11083	0.11997	0.01012	0.02095	0.32178	0.34549	0.52243	0.37658
16	189.45661	214.29585	197.38094	183.40326	0.01374	0.12580	0.09926	0.03047	0.78684	0.34267	0.23999	0.35596
17	202.44109	172.79875	161.87937	181.09274	0.19086	0.04207	0.02975	0.06261	0.37984	0.34929	0.58742	0.43287
18	217.08464	190.87659	211.26450	208.42294	0.02926	0.04668	0.09086	0.08305	0.50828	0.35388	0.42467	0.44111
19	210.71077	175.48246	164.83806	176.80389	0.06906	0.15397	0.07881	0.09680	0.36953	0.49049	0.61475	0.37454
20	208.22603	199.85642	196.20565	173.75774	0.50969	0.05924	0.20061	0.10330	0.63701	0.37300	0.36895	0.35456
21	200.53581	204.88963	217.80389	205.81863	0.12825	0.14843	0.19203	0.10577	0.27959	0.35382	0.26583	0.34870
22	194.01195	198.12027	162.42607	163.46021	0.08910	0.25994	0.08523	0.10565	0.35280	0.35715	0.56715	0.34896
23	136.84098	124.68503	109.46968	130.82969	0.13914	0.05457	0.08421	0.10422	0.27404	0.37629	0.67556	0.35228
24	136.98849	137.08238	129.72891	110.88337	0.11695	0.21990	0.05743	0.10171	0.27545	0.84122	0.51979	0.35881
Total	3801.54285	3786.28520	3665.15619	3466.33824	2.14624	2.54206	2.00160	1.73079	11.23356	11.69685	12.15234	10.02232

The open switches of four algorithms are shown in Table 17. The results are compared with those of the PSO, BAS, and BSO algorithms in Table 18 and Fig.29.

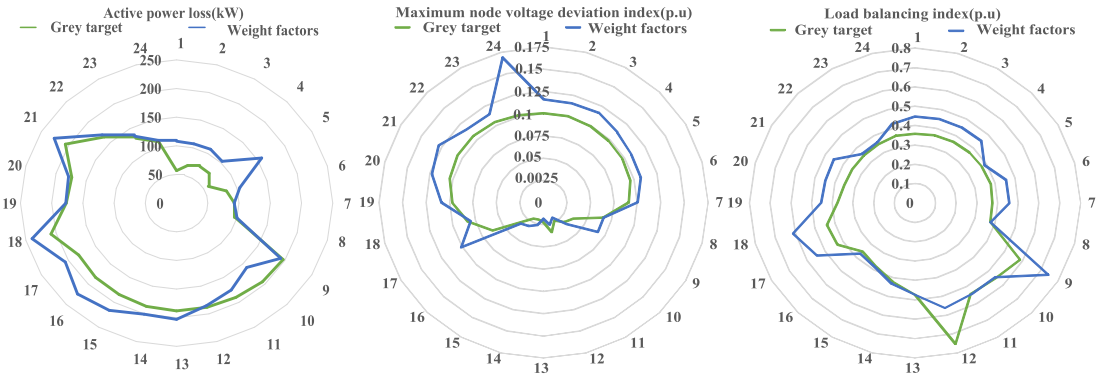

(a)Active power loss(kW). (b) Maximum node voltage deviation(p.u). (c) Load balancing(p.u).

FIGURE 28. The results of two methods based on IEEE-69 nodes.

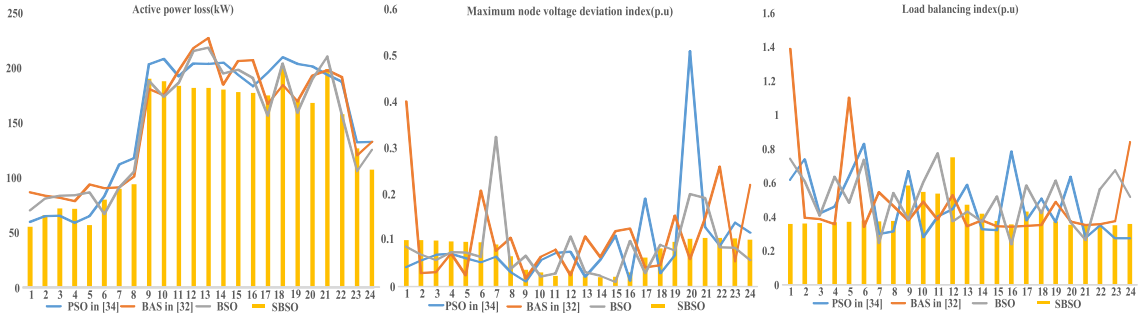

(a)Active power loss(kW). (b) Maximum node voltage deviation(p.u). (c) Load balancing(p.u).

FIGURE 29. Detail comparison based on IEEE-69 node with PSO, BAS, BSO algorithm.

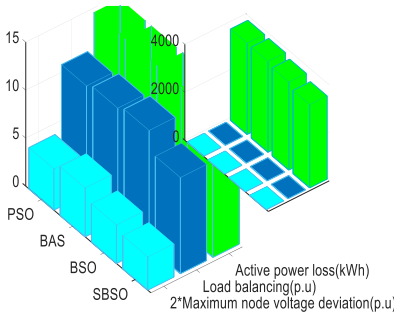

FIGURE 30. The results based on IEEE-69 node.

Table 18 and Fig.29 show that SBSO and BSO have smaller values than those of BAS and PSO. Although the results obtained by SBSO algorithm is not the smallest in 24 hours, which is related to the power grid state at that time, it can be seen from the Fig.29 that the results by SBSO algorithm is almost under the other values, and its value is optimal.

Table 19 and Fig.30 show that the SBSO and BSO have smaller values than those of BAS and PSO, and Fig.31 shows that the SBSO more easily finds smaller global optimal solutions in a shorter time. And the number of iterations of SBSO is significantly less than those of other three algorithms, which means the computation cost of the proposed approach is the least. These results indicate that the SBSO algorithm in this paper is also useful for IEEE-69 node. Therefore, the presented method is scalable.

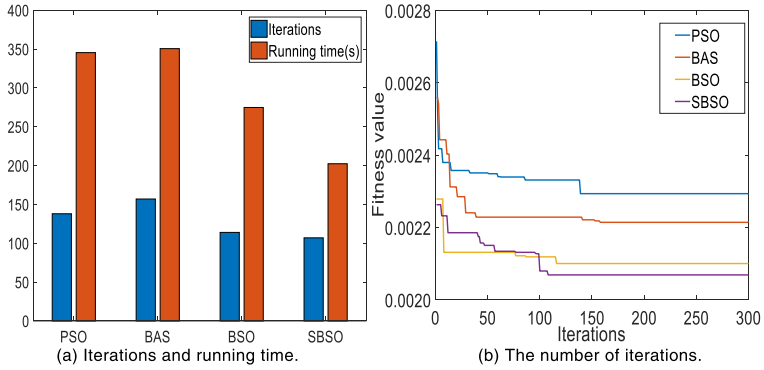

(a) Iterations and running time. (b) The number of iterations.

FIGURE 31. The computation cost based on IEEE-69 node.

TABLE 19. The results based on IEEE-69 node compared with PSO, BAS, BSO algorithm.

Algorithm	Active power loss(kWh)	Maximum node voltage deviation index(p.u)	Load balancing index(p.u)	Iterations	Running time(s)
PSO in [34]	3801.543	2.14624	11.23356	138	345.4674
BAS in [32]	3786.285	2.54206	11.69685	157	350.5965
BSO	3665.156	2.00160	12.15234	114	274.8609
SBSO	3466.338	1.73079	10.02232	107	202.4119

VII. CONCLUSION

Since a large number of distributed generation and complex load are connected to the distribution network, the safe and economic operation of the network is affected. In this paper, a multiobjective reconfiguration model of the distribution network considering wind power, solar power, and load is implemented for minimizing the sum of active power loss, the load balancing index, and the maximum node voltage deviation. In addition, SBSO based on a GTDM strategy was designed to solve the multiobjective optimization problem. Moreover, the grey correlation clustering method is utilized to divide the time period of DNRC in order to reduce the number of switching operations.

Here, proper DG access to the distribution network not only helps to absorb renewable energy but also improves the performance of distribution network indicators. At the same time, distribution network reconfiguration technology is also a very useful tool to reduce active power loss, improve the node voltage level, minimize load balancing. Additionally, the GRP method can effectively segment the time period of DNRC according to the randomness caused by DG and load in a day. Compared with the Entropy method, the SBSO based on GTDM strategy can achieve the goal of optimizing multiple indexes in the distribution network simultaneously. Moreover, the SBSO algorithm in this paper can effectively solve the complex multidimensional distribution network reconfiguration problem, and compared with the PSO, BAS, and BSO algorithms, it is more accurate and efficient.

REFERENCES

[1] W. Zheng, W. Huang, and D. J. Hill, "A deep learning-based general robust method for network reconfiguration in three-phase unbalanced active distribution networks," *Int. J. Electr. Power Energy Syst.*, vol. 120, Sep. 2020, Art. no. 105982, doi: 10.1016/j.ijepes.2020.105982.

[2] I. Benitez Cattani, E. Chaparro, and B. Baran, "Distribution system operation and expansion planning using network reconfiguration," *IEEE Latin Amer. Trans.*, vol. 18, no. 5, pp. 845–852, May 2020, doi: 10.1109/TLA.2020.9082912.

[3] I. A. Quadri, S. Bhowmick, and D. Joshi, "Multi-objective approach to maximise loadability of distribution networks by simultaneous reconfiguration and allocation of distributed energy resources," *IET Gener., Transmiss. Distrib.*, vol. 12, no. 21, pp. 5700–5712, Nov. 2018, doi: 10.1049/iet-gtd.2018.5618.

[4] J. Payne, F. Gu, G. Razeghi, J. Brouwer, and S. Samuelsen, "Dynamics of high penetration photovoltaic systems in distribution circuits with legacy voltage regulation devices," *Int. J. Electr. Power Energy Syst.*, vol. 124, Jan. 2021, Art. no. 106388, doi: 10.1016/j.ijepes.2020.106388.

[5] J. Shukla, B. K. Panigrahi, and P. K. Ray, "Stochastic reconfiguration of distribution system considering stability, correlated loads and renewable energy based DGs with varying penetration," *Sustain. Energy, Grids Netw.*, vol. 23, Sep. 2020, Art. no. 100366, doi: 10.1016/j.segan.2020.100366.

[6] A. M. Imran, M. Kowsalya, and D. P. Kothari, "A novel integration technique for optimal network reconfiguration and distributed generation placement in power distribution networks," *Int. J. Electr. Power Energy Syst.*, vol. 63, pp. 461–472, Dec. 2014, doi: 10.1016/j.ijepes.2014.06.011.

[7] M. J. Quintero-Duran, J. E. Candelo-Becerra, and K. Cabana-Jimenez, "Distribution network reconfiguration with large number of switches solved by a modified binary bat algorithm and improved seed population," *Tehnički Vjesnik*, vol. 26, no. 5, pp. 1284–1291, Feb. 2019.

[8] A. O. Salau, Y. W. Gebru, and D. Bitew, "Optimal network reconfiguration for power loss minimization and voltage profile enhancement in distribution systems," *Heliyon*, vol. 6, no. 6, Jun. 2020, Art. no. e04233, doi: 10.1016/j.heliyon.2020.e04233.

[9] D. Jakus, R. Čaenović, J. Vasilj, and P. Sarajčev, "Optimal reconfiguration of distribution networks using hybrid heuristic-genetic algorithm," *Energies*, vol. 13, no. 7, p. 1544, Mar. 2020, doi: 10.3390/en13071544.

[10] A. Azizivahed, A. Arefi, S. Ghavidel, M. Shafie-khah, L. Li, J. Zhang, and J. P. S. Catalao, "Energy management strategy in dynamic distribution network reconfiguration considering renewable energy resources and storage," *IEEE Trans. Sustain. Energy*, vol. 11, no. 2, pp. 662–673, Apr. 2020, doi: 10.1109/TSTE.2019.2901429.

[11] P. P. Biswas, P. N. Suganthan, B. Y. Qu, and G. A. J. Amaratunga, "Multiobjective economic-environmental power dispatch with stochastic wind-solar-small hydro power," *Energy*, vol. 150, pp. 1039–1057, May 2018, doi: 10.1016/j.energy.2018.03.002.

[12] Y. Yin, T. Liu, and C. He, "Day-ahead stochastic coordinated scheduling for thermal-hydro-wind-photovoltaic systems," *Energy*, vol. 187, Nov. 2019, Art. no. 115944, doi: 10.1016/j.energy.2019.115944.

[13] V. K. Jadoun, V. C. Pandey, N. Gupta, K. R. Niazi, and A. Swarnkar, "Integration of renewable energy sources in dynamic economic load dispatch problem using an improved fireworks algorithm," *IET Renew. Power Gener.*, vol. 12, no. 9, pp. 1004–1011, Jul. 2018, doi: 10.1049/iet-rpg.2017.0744.

[14] H. Teimourzadeh and B. Mohammadi-Ivatloo, "A three-dimensional group search optimization approach for simultaneous planning of distributed generation units and distribution network reconfiguration," *Appl. Soft Comput.*, vol. 88, Mar. 2020, Art. no. 106012, doi: 10.1016/j.asoc.2019.106012.

[15] M. Esmaeili, M. Sedighizadeh, and M. Esmaili, "Multi-objective optimal reconfiguration and DG (distributed generation) power allocation in distribution networks using big bang-big crunch algorithm considering load uncertainty," *Energy*, vol. 103, pp. 86–99, May 2016, doi: 10.1016/j.energy.2016.02.152.

[16] J. Zhao, H. Niu, and Y. Wang, "Dynamic reconfiguration of active distribution network based on information entropy time division," *Power Syst. Technol.*, vol. 41, no. 2, pp. 402–408, Feb. 2017, doi: 10.13335/j.1000-3673.pst.2016.2381.

[17] D. Jiang, T. Liu, and F. Li, "Dynamic distribution network reconfiguration based on dynamic partition of time intervals and hierarchical optimization," *Power Syst. Technol.*, vol. 36, no. 2, pp. 153–157, 2012, doi: 10.13335/j.1000-3673.pst.2012.02.030.

[18] C. Yu, T. Wei, X. Chen, P. Cong, and Z. Lu, "Tie switch allocation optimization based on dynamic segment of equivalent load-PV curve," *Electr. Power Autom. Equip.*, vol. 35, pp. 47–53, Mar. 2015.

[19] Z. Dong and L. Lin, "Dynamic reconfiguration strategy based on partition of time intervals with improved fuzzy C-means clustering," in *Proc. China Int. Conf. Electr. Distrib. (CICED)*, Sep. 2018, pp. 398–404, doi: 10.1109/CICED.2018.8592081.

[20] Y. Li, B. Feng, G. Li, J. Qi, D. Zhao, and Y. Mu, "Optimal distributed generation planning in active distribution networks considering integration of energy storage," *Appl. Energy*, vol. 210, pp. 1073–1081, Jan. 2018, doi: 10.1016/j.apenergy.2017.08.008.

[21] Y. Li, Y. Li, G. Li, D. Zhao, and C. Chen, "Two-stage multi-objective OPF for AC/DC grids with VSC-HVDC: Incorporating decisions analysis into optimization process," *Energy*, vol. 147, pp. 286–296, Mar. 2018, doi: 10.1016/j.energy.2018.01.036.
[22] Y. Li, Z. Yang, D. Zhao, H. Lei, B. Cui, and S. Li, "Incorporating energy storage and user experience in isolated microgrid dispatch using a multi-objective model," *IET Renew. Power Gener.*, vol. 13, no. 6, pp. 973–981, Apr. 2019, doi: 10.1049/iet-rpg.2018.5862.
[23] J. P. Avilés, J. C. Mayo-Maldonado, and O. Micheloud, "A multi-objective evolutionary approach for planning and optimal condition restoration of secondary distribution networks," *Appl. Soft Comput.*, vol. 90, May 2020, Art. no. 106182, doi: 10.1016/j.asoc.2020.106182.
[24] Q. Lu, L. Chen, and S. Mei, "Typical applications andprospects of game theory in power system," *Proc. CSEE*, vol. 34, no. 29, pp. 5009–5017, Feb. 2014.
[25] S. Ganguly, N. C. Sahoo, and D. Das, "Multi-objective planning of electrical distribution systems using dynamic programming," *Int. J. Electr. Power Energy Syst.*, vol. 46, pp. 65–78, Mar. 2013, doi: 10.1016/j.ijepes.2012.10.030.
[26] H. Khazraj, B. Y. Khanghah, P. Ghimire, F. Martin, M. Ghomi, F. Faria da Silva, and C. Leth Bak, "Optimal operational scheduling and reconfiguration coordination in smart grids for extreme weather condition," *IET Gener., Transmiss. Distrib.*, vol. 13, no. 15, pp. 3455–3463, Aug. 2019, doi: 10.1049/iet-gtd.2019.0507.
[27] M. H. R. Nascimento, M. V. A. Nunes, J. L. M. Rodríguez, and J. C. Leite, "A new solution to the economical load dispatch of power plants and optimization using differential evolution," *Elect. Eng.*, vol. 99, no. 2, pp. 1–11, 2016, doi: 10.1007/s00202-016-0385-2.
[28] Y. Li, J. Wang, D. Zhao, G. Li, and C. Chen, "A two-stage approach for combined heat and power economic emission dispatch: Combining multi-objective optimization with integrated decision making," *Energy*, vol. 162, pp. 237–254, Nov. 2018, doi: 10.1016/j.energy.2018.07.200.
[29] Y. G. Dong and S. F. Liu, *Grey System Theory and its Application*. BeiJing, China: Science Press, 2014, pp. 256–261.
[30] G. Zhang, W. Wang, J. Du, and H. Liu, "A multiobjective optimal operation of a stand-alone microgrid using SAPSO algorithm," *J. Electr. Comput. Eng.*, vol. 2020, pp. 1–16, Mar. 2020, doi: 10.1155/2020/6042105.
[31] M. Zhang and Y. Li, "Multi-objective optimal reactive power dispatch of power systems by combining classification-based Multi-objective evolutionary algorithm and integrated decision making," *IEEE Access*, vol. 8, pp. 38198–38209, 2020, doi: 10.1109/ACCESS.2020.2974961.
[32] Z. Zhu, Z. Zhang, W. Man, X. Tong, J. Qiu, and F. Li, "A new beetle antennae search algorithm for multi-objective energy management in microgrid," in *Proc. 13th IEEE Conf. Ind. Electron. Appl. (ICIEA)*, May 2018, pp. 1599–1603, doi: 10.1109/ICIEA.2018.8397965.
[33] X. Jiang and S. Li, "BAS: Beetle antennae search algorithm for optimization problems," 2017, *arXiv:1710.10724*. [Online]. Available: http://arxiv.org/abs/1710.10724
[34] H. S. Ramadan, A. F. Bendary, and S. Nagy, "Particle swarm optimization algorithm for capacitor allocation problem in distribution systems with wind turbine generators," *Int. J. Electr. Power Energy Syst.*, vol. 84, pp. 143–152, Jan. 2017, doi: 10.1016/j.ijepes.2016.04.041.
[35] X. Li, W. Wang, H. Wang, J. Wu, X. Fan, and Q. Xu, "Dynamic environmental economic dispatch of hybrid renewable energy systems based on tradable green certificates," *Energy*, vol. 193, Feb. 2020, Art. no. 116699.
[36] J. Wang, W. Wang, Z. Yuan, H. Wang, and J. Wu, "A chaos disturbed beetle antennae search algorithm for a multiobjective distribution network reconfiguration considering the variation of load and DG," *IEEE Access*, vol. 8, pp. 97392–97407, 2020, doi: 10.1109/ACCESS.2020.2997378.
[37] M. R. Dorostkar-Ghamsari, M. Fotuhi-Firuzabad, M. Lehtonen, and A. Safdarian, "Value of distribution network reconfiguration in presence of renewable energy resources," *IEEE Trans. Power Syst.*, vol. 31, no. 3, pp. 1879–1888, May 2016.
[38] X. Jiang and S. Li, "Beetle antennae search without parameter tuning (BAS-WPT) for multi-objective optimization," 2017, *arXiv:1711.02395*. [Online]. Available: http://arxiv.org/abs/1711.02395
[39] M. E. Baran and F. F. Wu, "Network reconfiguration in distribution systems for loss reduction and load balancing," *IEEE Trans. Power Del.*, vol. 4, no. 2, pp. 1401–1407, Apr. 1989, doi: 10.1109/61.25627.
[40] Y. Zheng, X. Fu, and Y. Xuan, "Active distribution network reconfiguration considering distributed generation and load uncertainty," *J. Shanghai Inst. Electr. Eng.*, vol. 22, no. 5, pp. 262–269, 2019.
[41] M. Lin and Q. Li, "A hybrid optimization method of beetle antennae search algorithm and particle swarm optimization," in *Proc. Int. Conf. Elect., Control, Automat. Robot. (ECAR)*, Xiamen, China, Sep. 2018, pp. 396–401, doi:10.12783/dtetr/ecar2018/26379.
[42] J. Wang and H. Chen, "BSAS: Beetle swarm antennae search algorithm for optimization problems," 2018, *arXiv:1807.10470*. [Online]. Available: http://arxiv.org/abs/1807.10470
[43] C. Li, S. Yang, and T. Thanh Nguyen, "A self-learning particle swarm optimizer for global optimization problems," *IEEE Trans. Syst., Man, Cybern. B, Cybern.*, vol. 42, no. 3, pp. 627–646, Jun. 2012.
[44] V. Vahidinasab, M. Tabarzadi, H. Arasteh, M. I. Alizadeh, M. Mohammad Beigi, H. R. Sheikhzadeh, K. Mehran, and M. S. Sepasian, "Overview of electric energy distribution networks expansion planning," *IEEE Access*, vol. 8, pp. 34750–34769, 2020, doi: 10.1109/ACCESS.2020.2973455.
[45] B. Mukhopadhyay and D. Das, "Multi-objective dynamic and static reconfiguration with optimized allocation of PV-DG and battery energy storage system," *Renew. Sustain. Energy Rev.*, vol. 124, May 2020, Art. no. 109777, doi: 10.1016/j.rser.2020.109777.
[46] M. B. Shafik, H. Chen, G. I. Rashed, R. A. El-Sehiemy, M. R. Elkadeem, and S. Wang, "Adequate topology for efficient energy resources utilization of active distribution networks equipped with soft open points," *IEEE Access*, vol. 7, pp. 99003–99016, 2019, doi: 10.1109/ACCESS.2019.2930631.
[47] J. Zhang, Y. Cao, Y. Li, and L. Zhang, "Aeroengine health monitoring method based on improved grey target theory," *J. Vib. Meas. Diagnosis*, vol. 38, no. 2, pp. 228–233, Apr. 2018, doi: 10.16450/j.cnki.issn.1004-6801.2018.02.002.

QIAN CHEN received the B.E. degree in electric power systems and automation from Xinjiang University, Urumqi, China, in 2017, where she is currently pursuing the Ph.D. degree with the Engineering Research Center of Renewable Energy Power Generation and Grid-Connected Control, Ministry of Education. Her current research interests include control of renewable energy power generation and smart grid technology.

WEIQING WANG received the B.E. degree in electric power systems and automation from the Xinjiang Institute of Technology, Urumqi, China, in 1983, and the M.E. degree in electric power systems and automation from Zhejiang University, Hangzhou, China, in 1990. He is currently a Professor with the Engineering Research Center of Renewable Energy Power Generation and Grid-Connected Control, Ministry of Education, Xinjiang University. His current research interests include control of renewable energy power generation and smart grid technology.

HAIYUN WANG received the B.E. degree in electric power systems and automation from Xinjiang University, Urumqi, China, in 1995, and the M.E. degree in electrical engineering from the Dalian University of Technology, Liaoning, China, in 1999. She is currently a Professor with the Engineering Research Center of Renewable Energy Power Generation and Grid-Connected Control, Ministry of Education, Xinjiang University. Her current research interests include control of renewable energy power generation and smart grid technology.

JIAHUI WU received the B.E. degree in chemical technology and automation from the Beijing University of Chemical Technology, Beijing, China, in 2011, and the Ph.D. degree in electric power systems and automation from Xinjiang University, Urumqi, China, in 2018. She is currently an Associate Professor with the Engineering Research Center of Renewable Energy Power Generation and Grid-Connected Control, Ministry of Education, Xinjiang University. Her current research interests include control of renewable energy power generation and smart grid technology.

XIAOZHU LI received the B.E. degree in measurement and control technology and instruments from the Changsha University of Technology, in 2013, and the M.E. degree in control science and control engineering from Xinjiang University, China, in 2017, where she is currently pursuing the Ph.D. degree with the Department of Electrical Engineering.

JIONGFENG LAN received the B.E. degree in human resource management from North Minzu University, Yinchuan, China, in 2018. He is currently pursuing the M.E. degree with the International Business Management, Newcastle University. His current research interest includes electricity market analysis.